

Generalized and Personalized Federated Learning with Foundation Models via Orthogonal Transformations

Eun Gyung Kong* Je Won Yeom* Yonghoon Jeon Taesup Kim†
Graduate School of Data Science, Seoul National University

Abstract

Federated Learning (FL) aims to train models across decentralized clients or devices holding local data without the need for centralized data collection, thus enhancing data privacy and security. However, achieving both generalization and personalization in heterogeneous settings remains a significant challenge. To address this, we introduce FedOT, a novel approach that leverages black-box foundation models. FedOT shares only a global task-dependent classifier across clients while locally adapting features through orthogonal transformations. By enforcing orthogonality, FedOT mitigates gradient conflicts across diverse clients, preserves semantic integrity, and achieves robust performance even in the presence of substantial data heterogeneity. The strategy of combining global and local parameters enables a more balanced approach for both generalization and personalization, outperforming baseline FL methods across multiple benchmarks. Furthermore, our extensive analysis confirms that joint optimization of global classifiers and local orthogonal transformations yields superior performance and suggests broader applicability.

1 Introduction

The advancement of deep learning has underscored the importance of leveraging large-scale datasets, yet data collection is often constrained by privacy and security concerns. Federated Learning (FL) offers a promising alternative by enabling decentralized model training across distributed clients without requiring centralized data aggregation [39, 40, 51]. The primary objective of FL is to develop a unified and generalized model that performs well across all participating clients. Furthermore, the goal of generalization within FL extends to learning a shared model that remains effective not only for current clients but also for future, unseen ones. However, variations in data distributions across clients (i.e., the non-IID setting) often necessitate personalized models rather than relying solely on a single generalized model. This requirement is particularly critical in domains such as healthcare [49, 16] and recommendation systems [76], where personalized models trained through FL are essential to provide high-quality services. As a result, there is a growing demand for FL models that effectively balance generalization and personalization. Despite this need, most existing approaches tend to prioritize one aspect over the other. Achieving this balance within the FL framework presents a significant challenge, akin to simultaneously addressing domain generalization and domain adaptation.

Recently, foundation models [5], including pre-trained vision models and vision-language models (VLMs), have demonstrated strong generalization capabilities, exhibiting promising scalability and performance across various vision downstream tasks. This makes the integration of foundation models into FL particularly compelling. For instance, encoders from VLMs, such as CLIP [65], possess inherent zero-shot capabilities and strong generalization, which can significantly enhance

*Equal contribution.

†Corresponding author.

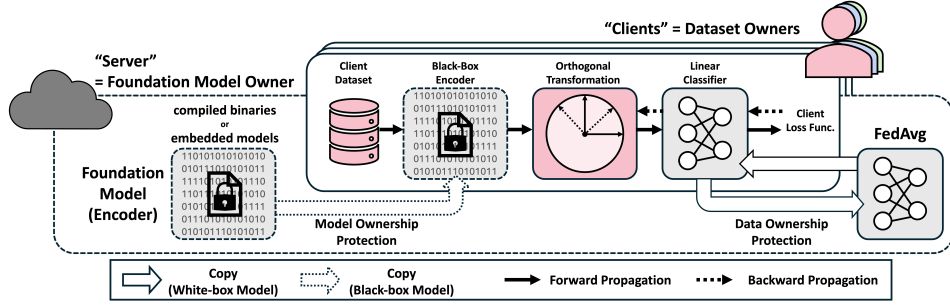


Figure 1: **Overview of our proposed FL framework.** FEDOT leverages the pre-trained vision encoder into an FL environment. The image encoder, deployed in binary or embedded formats, operates with orthogonal transformation used in the local parameters for client-specific personalization, while holding a globally shared classifier. Through federated updates, our method strikes a balance between personalization and generalization, preserving both data privacy and model intellectual property.

the efficiency of FL. Inspired by this potential, in this paper, we tackle key challenges in FL by leveraging a pre-trained foundation model, specifically the vision encoder from CLIP, with the goal of simultaneously achieving both generalization and personalization.

We propose FEDOT, a simple yet effective FL framework in which clients share and communicate only a task-dependent classifier while locally transforming visual features using orthogonal transformations instead of fine-tuning the vision encoder’s parameters. This approach enables a FL on black-box foundation model, ensuring both model security from the server’s perspective (as the model provider) and data security from the clients’ perspective (as data providers) [77]. Unlike existing methods [64, 46], which require access to the model architecture and involve modifying the internal parameters of pre-trained models, our method modifies only the final visual feature space through orthogonal transformations. Crucially, orthogonal transformations allow FEDOT to mitigate gradient conflicts across heterogeneous clients, preserve the semantic properties of foundation model representations, and maintain robust performance even under significant data heterogeneity. Notably, we show that orthogonal transformations, which are linear feature transformations with a condition number of 1 ($\kappa = 1$), achieve the smallest upper bound on gradient discrepancy across clients, thereby enhancing generalization. Our extensive evaluation demonstrates that FEDOT consistently delivers strong personalization performance and confirms that orthogonality provides better generalization than unconstrained linear transformations.

The contributions of our framework can be summarized in three ways:

- To the best of our knowledge, this work is the first to demonstrate the effectiveness of Orthogonal Transformation in mitigating gradient conflicts within the context of FL. We leverage this property to efficiently harness the generalization capabilities of foundation models while simultaneously adapting client models to their unique data distributions for personalization.
- Additionally, our framework integrates orthogonal transformations with a pre-trained image encoder (i.e., a vision foundation model), ensuring secure operation in FL environments. This design safeguards the intellectual property of the foundation model provider (server) while simultaneously protecting the data privacy of the participants (clients).
- Our framework is built upon rigorous theoretical analysis and validated through extensive empirical evaluations. It consistently surpasses existing approaches in terms of generalization, personalization, and comprehensive performance, demonstrating its broad applicability across diverse datasets.

2 Related Work

In this section, we introduce three key topics. A more comprehensive discussion of related works on foundation models and federated learning is provided in Appendix A.

Domain Generalization and Domain Adaptation. Domain Generalization (DG) and Domain Adaptation (DA) enhance model robustness to distribution shifts across related domains. DG trains on multiple source domains and must generalize to unseen targets without accessing their data during training [32]. State-of-the-art DG relies on domain-invariant representations [53, 54], meta-learning schemes [3, 43], and data-augmentation generators that synthesize novel styles [68, 55]. DA, in contrast, fine-tunes source-pre-trained models using limited target data [24]. It spans supervised [73], unsupervised [26], and semi-supervised [78] settings, with methods broadly grouped into discrepancy-based [47, 70], reconstruction-based [28, 6], and adversarial-based [62] approaches. Recent work blurs the DG/DA boundary by performing online test-time adaptation [13, 17]. Yet most solutions still assume centralized data access, a limitation now challenged by Federated DG frameworks [82, 29].

Transformation with Orthogonality. Recent studies have explored methods that leverage orthogonality for fine-tuning pre-trained models. PRO² [12] employs a linear projection with an orthonormal basis to map pre-trained embeddings from a source dataset onto orthogonal directions, ensuring label predictability. This method then trains a linear classifier on the projected features using a small target dataset. Similarly, Qiu and Liu [64, 46] propose Orthogonal Fine-Tuning (OFT), which fine-tunes foundation models by reparameterizing pre-trained weights with orthogonal matrices instead of using LoRA [36] adapters. They demonstrate that OFT preserves the semantics from foundation models by maintaining hyper-spherical energy, thus preventing the destruction of pre-trained information. While OFT methods effectively adapt foundation models, they require access to the model architecture and involve modifications to the internal mechanisms of pre-trained models. In contrast, our novel approach maps an orthogonal transformation externally to the encoder, transforming the embedding space while applying the black-box nature to the models.

Black-Box Foundation Model and Federated Learning. Foundation models have achieved remarkable success in various domains [5]. However, practical scenarios frequently enforce black-box interactions due to intellectual property protection, proprietary software policies, restrictions in API access, or privacy concerns [71, 80, 59]. Common black-box adaptation methods include gradient-free prompt tuning techniques [71, 80, 52], the integration of external lightweight wrappers [57, 9, 83], and embedding-based feature transformations relying solely on precomputed embeddings [58, 56, 77, 34]. In Federated learning (FL), BlackFed [60] defines the concept of black-box FL, where clients interact with a global model solely through outputs of two-layer convolution network under strict black-box conditions, which focuses on model security, yet overlooks multi-client personalization challenges. ZooPFL [50] introduces black-box foundation FL, in distinction to black-box FL introduced in BlackFed [60], addressing resource limitations and personalization by adapting inputs via zeroth-order optimization with black-box foundation models. Meanwhile, our method uniquely employs orthogonal transformations fully decoupled from foundation models in FL, which precisely belongs to black-box foundation FL, effectively supporting both personalization and generalization.

3 Method

We propose FedOT, a simple yet parameter-efficient approach for FL that preserves data privacy and protects proprietary foundation models while effectively enhancing both generalization and personalization. By leveraging orthogonal transformations, our method enhances generalization across diverse clients while enabling local adaptation to non-IID data distributions.

3.1 Generalization and Personalization in FL

We clarify the fundamental concepts of generalization and personalization in FL, with reference to FedCLIP [48]. We consider an FL scenario where diverse clients with unique data distributions participate, emphasizing the need for personalization, while new, unseen clients are expected to join after the learning process concludes, underscoring the need for generalization. Based on this premise, we aim to evaluate performance not only from the perspective of clients actively participating in FL but also in terms of its applicability to future, unseen clients. This evaluation directly corresponds to personalization and generalization, respectively, highlighting their critical roles in assessing the FL model’s adaptability and robustness across diverse and evolving client environments.

3.2 Global and Local Parameters

FedOT integrates both global and local parameters within the FL setting, leveraging the generalization capabilities of pre-trained foundation models without requiring explicit fine-tuning of their internal parameters, as depicted in Figure 1. Specifically, we assume a black-box vision foundation model shared across all clients, serving as a fixed image encoder. In parallel, we introduce client-specific local parameters in the form of *orthogonal transformations* that personalize representations, leaving the underlying foundation model unchanged. To support a vision downstream task, we introduce a *global classifier* collaboratively trained and shared among clients to enhance generalization. While the classifier can be randomly initialized, it may also be initialized with text features from a vision-language model (VLM) like CLIP, to potentially improve performance. This dual approach, jointly optimizing global and local parameters, strikes a balance between generalization across heterogeneous clients and personalization tailored to each client’s unique data distribution.

The global parameters are represented by a task-dependent linear classifier $w_g \in \mathbb{R}^{K \times d}$, where K and d denote the number of classes and the dimensionality of the feature space, respectively. As mentioned, they can be randomly initialized or derived from a set of class embeddings $t = \{\mathcal{T}(p_c)\}_{c=1}^K$, where p_c is a class-specific text prompt and \mathcal{T} is the text encoder of CLIP. For each client $i \in 1, 2, \dots, N$, the local parameters $w_1^{(i)} \in \mathbb{R}^{d \times d}$ are kept and updated locally, and these parameters on the server side are fixed as the identity matrix $I \in \mathbb{R}^{d \times d}$ throughout the FL process. The combined parameter notation for each client i is $W^{(i)} = \{w_g^{(i)}, w_1^{(i)}\}$. An ablation study in Section 5.3 investigates the impact of global and local parameters in our framework.

Orthogonal Transformations. Orthogonal transformation refers to a linear operation that preserves the geometric properties of the vector space, specifically the lengths of vectors and the angles between them. In machine learning contexts, applying an orthogonal transformation to a feature space allows one to adapt the representation without distorting its underlying manifold, thus retaining the semantic integrity of the original features.

3.3 Parameter Update

Once clients join the FL process, synchronization with the server is initiated. During the initialization phase, each client is configured to use a shared vision foundation model $\mathcal{I}(\cdot)$, with global parameters initialized to the server’s values $w_g^{(i)} \leftarrow w_g$ and local parameters set to the identity matrix $w_1^{(i)} \leftarrow I$. Following initialization, each client updates its trainable parameters based on its local data distribution. The updated global parameters from all clients are then aggregated on the server using a standard FL approach, such as FedAvg [51]. Meanwhile, each client i holds a set of local parameters $w_1^{(i)}$, which serve as a learnable *orthogonal transformation* in FedOT. This transformation allows the model to adapt to client-specific characteristics while leveraging the feature representation of the vision foundation model.

Each client utilizes the classification probability to optimize its local updates. Specifically, the original visual feature $h = \mathcal{I}(x)$ is linearly transformed into $h' = w_1^{(i)} h$, where $w_1^{(i)}$ is constrained to be an orthogonal matrix, ensuring that the core feature representation is preserved while adapting to the unique data distribution of each client. For each client i , the classification probability is given by $P(y | x; w_g, w_1^{(i)}) = \text{softmax} \left(\tau w_g \left(w_1^{(i)} \mathcal{I}(x) / \|w_1^{(i)} \mathcal{I}(x)\| \right) \right)$, where τ is a temperature value, and the transformed feature h' is first normalized before being passed through the linear classifier w_g . The softmax function is then applied to convert the resulting logits into class probabilities. In particular, each client i aims to minimize the following cross-entropy loss:

$$\ell^{(i)}(w_g^{(i)}, w_1^{(i)}) = \mathbb{E}_{(x,y) \sim D^{(i)}} [-\log P(y | x; w_g^{(i)}, w_1^{(i)})],$$

where $D^{(i)}$ is a labeled dataset representing the unique data distribution of client i .

Algorithm of FedOT. Here, we specify the algorithm of FedOT. Initially, the server shares its learnable global parameter w_g and sets the local transform to the identity I . On the client side, let $X^{(i)}$ be an unconstrained matrix, initialized to the identity I , from which $w_1^{(i)}$ is derived via a differentiable *Cayley transform* to ensure orthogonality. Specifically, $w_1^{(i)} = (I + R^{(i)}) (I - R^{(i)})^{-1}$

, where $R^{(i)} = \frac{1}{2} \left(X^{(i)} - (X^{(i)})^\top \right)$. During local training, the parameters are updated with respect to a sampled mini-batch over several epochs as $w_g^{(i)} \leftarrow w_g^{(i)} - \eta \nabla_{w_g^{(i)}} \ell^{(i)}(w_g^{(i)}, w_1^{(i)})$ and $X^{(i)} \leftarrow X^{(i)} - \eta \nabla_{X^{(i)}} \ell^{(i)}(w_g^{(i)}, w_1^{(i)})$, then $w_1^{(i)}$ is recomputed from $X^{(i)}$ via the Cayley transform to maintain orthogonality.

After local training, the server gathers the updated *global* parameters from the clients (i.e., $\{w_g^{(i)}\}$) and updates as $w_g \leftarrow \frac{1}{N} \sum_{i=1}^N w_g^{(i)}$, where N is the number of participating clients. Finally, each client i receives the updated global parameter w_g from the server and sets as $w_g^{(i)} \leftarrow w_g$, which completes one communication round. Refer to Algorithm 1 for the pseudo-code.

3.4 Protecting Proprietary Models and Data

Preserving the intellectual property of foundation models and protecting data ownership are critical concerns for model providers and data owners, respectively. Our framework ensures data privacy by operating within an FL setting, where raw data remains on local devices and only model updates are exchanged. This setup inherently protects user data privacy. Furthermore, transforming the extracted image features enables adaptation without accessing or modifying the internal parameters of the image encoder. This allows the image encoder to function as a black-box module, facilitating the deployment of foundation models in binary or embedded formats without exposing proprietary weights. Thus, FedOT serves to protect both the foundation model and the data, offering tangible benefits for building secure and deployable distributed learning systems. For a more in-depth comparison of learning frameworks and their applications, refer to Table 4.

4 Theoretical Analysis of FedOT

In this section, we present key theoretical insights behind FedOT, demonstrating how enforcing orthogonality on local parameters $w_1^{(i)}$ mitigates gradient conflicts among heterogeneous clients, thereby balancing personalization and generalization.

4.1 Bounding the Gradient Difference Between Clients

Recall that each client i transforms the visual feature $h = \mathcal{I}(x)$ into $h' = w_1^{(i)} h$. We then measure the cross-entropy loss $\ell^{(i)}(w_g^{(i)}, w_1^{(i)})$ and compute a standard derivative with respect to $w_g^{(i)}$:

$$\nabla_{w_g^{(i)}} \ell^{(i)} = \mathbb{E} \left[\tau(r_x^{(i)} - y) \left(\frac{h'}{\|h'\|} \right)^\top \right],$$

where $r_x^{(i)}$ corresponds to the classification probability $P(y | x; w_g^{(i)}, w_1^{(i)})$. Based on this, we now investigate how the difference of these gradients across two distinct clients i and j can be bounded.

Theorem 4.1. (*Gradient Difference Bound*) *Let i and j be two distinct clients. Then the ℓ_2 -norm of the difference between their global-parameter gradients satisfies*

$$\left\| \nabla_{w_g^{(i)}} \ell^{(i)} - \nabla_{w_g^{(j)}} \ell^{(j)} \right\| \leq 2\tau \left[\kappa(w_1^{(i)}) + \kappa(w_1^{(j)}) \right],$$

where $\kappa(\cdot)$ is the condition number of the corresponding linear transformation. Moreover, if $\kappa(w_1^{(i)}) = \kappa(w_1^{(j)}) = 1$, then the bound becomes 4τ , which is the smallest value possible. For a detailed proof, see Appendix E.

Implications. This theorem indicates that if each local linear transformation $w_1^{(i)}$ is *orthogonal* (hence $\kappa = 1$), the gradient mismatch among clients is tightly bounded by 4τ . Thus, orthogonality *directly* reduces gradient conflicts between clients in FL, facilitating stable global parameters' updates even under heterogeneous clients (i.e., non-IID data distributions).

4.2 Benefits of Orthogonal Transformations

A matrix $Q \in \mathbb{R}^{d \times d}$ is orthogonal, if $Q^\top Q = I$. Moreover, all eigenvalues of Q lie on $\{\pm 1\}$, so $\kappa(Q) = 1$. (Refer to E.4.3 for the proof.) Hence, substituting $w_1^{(i)} = Q$ into Theorem 4.1 yields the

minimal possible mismatch bound of 4τ . This property preserves distances and angles in the visual feature space, preventing feature collapse while maintaining the semantic property of the pre-trained foundation model’s representation.

Geometric and Semantic Advantages. In addition to bounding gradient discrepancies, orthogonal transformations are invertible, thereby one-to-one, ensuring that distinct features $\{\mathcal{I}(x)\}$ remain distinct after transformation. Furthermore, an orthogonal matrix in $\mathbb{R}^{d \times d}$ has $\frac{d(d-1)}{2}$ degrees of freedom (DOF), approximately half that of a general linear transformation (d^2). This reduction in DOF helps preserve the structure of the pre-trained manifold, mitigating excessive distortion and reducing the risk of overfitting to local data.

4.3 Block-Diagonal Orthogonal Transformations

We can further reduce DOF via a *block-diagonal* design of orthogonal matrices. Partition the dimension d into r blocks, each block $Q_k \in \mathbb{R}^{d/r \times d/r}$ being orthogonal:

$$B = \text{diag}(Q_1, Q_2, \dots, Q_r), \quad B^\top B = I.$$

Since each Q_k is orthogonal, $\kappa(B) = 1$. This preserves the lowest bound in Theorem 4.1 while lowering the DOF to $r \times \frac{(d/r)(d/r-1)}{2} = \frac{d(d/r-1)}{2}$, potentially yielding a lighter yet still *orthogonally constrained* transform.

5 Experiments

5.1 Setup

Datasets & Baselines. We validate the robustness of our proposed method to domain heterogeneity by using five datasets, where each subset has unique domain characteristics: FEMNIST [8], PACS [42], Office-Home [74], VLCS [23], TerraIncognita [4]. These datasets range from simplistic, less complex toy datasets to real-world datasets that capture the intricacies of real-life scenarios.

We compare our method with CLIP’s zero-shot performance and other parameter-efficient fine-tuning approaches. Specifically, we introduce FedCLIP [48], which incorporates an adapter positioned behind the CLIP image encoder. For modality-wise prompt tuning in VLMs, we adopt PromptFL [33] based on CoOp [85], and implement CoCoOp [84] and VPT [38] within the federated setting. We also experimented FedAKT(C) and FedGH(C), a variant of FedAKT [45] and FedGH [79] that adopts CLIP as client models, to ensure a more fair comparison. Meanwhile, we include a variant of our method, treating all trainable parameters as global parameters, referred to as FedAVG. To further validate our approach, we introduce FedOT(+B), an extension which incorporates block-diagonal orthogonal transformations.

Additional details on the datasets and implementation are available in Appendix F.1.

Metrics. We evaluate the baselines and our method using generalization, personalization, and comprehensive accuracy. One domain is used as the test set, and this process is iteratively repeated for all domains.

Let $\text{ACC}_j^{(i)}$, where $i, j \in \{1, \dots, N\}$, denote the test accuracy of the i^{th} client when the j^{th} client is a test client. We define the following evaluation metrics to assess model performance [48]: (1) **Generalization** performance is quantified as $\frac{1}{N} \sum_{i=1}^N \text{ACC}_i^{(i)}$, evaluating how effectively the aggregated server model adapts to the test data of unseen clients. (2) **Personalization** performance is measured as $\frac{1}{N} \sum_{j=1}^N \frac{1}{N-1} \sum_{i \neq j} \text{ACC}_j^{(i)}$, which reflects the client model’s ability to perform well on its own domain after training. Finally, (3) **Comprehensive** performance is computed as $\frac{1}{N} \sum_j \frac{1}{N} \sum_i \text{ACC}_j^{(i)}$, which provides an overall measure of model performance by considering both generalization and personalization aspects. These metrics enable cross-validation experiments across all domains within each dataset, providing a holistic evaluation of model adaptability. In our experiments, we set $N = 4$, corresponding to the four clients (i.e., domains) in the datasets.

Table 1: **Overview of generalization, personalization, and comprehensive accuracies across five datasets.** The reported results for PromptFL, CoCoOp, and VPT correspond to their representative experiments. For more detailed results, refer to Appendix F.2. FedAVG refers to a variant of our method, treating all trainable parameters (e.g. classifiers, orthogonal transformation) as global parameters.

		FEMNIST	PACS	Office-Home	VLCS	TerraIncognita
Zero-Shot	CLIP	49.22	94.08	79.17	81.07	18.79
Generalization	PromptFL	96.73	94.61	81.28	81.64	39.72
	CoCoOp	12.48	89.04	74.11	54.68	31.57
	VPT	68.13	94.73	81.11	81.26	35.05
	FedAKT(C)	10.45	15.40	1.41	27.45	5.80
	FedGH(C)	37.90	54.80	1.64	41.92	9.73
	FedCLIP	80.07	94.61	80.15	81.41	34.33
	FedAVG	92.70	94.48	81.80	82.23	32.21
	FedOT	94.89	94.68	81.30	81.11	34.80
	FedOT(+B)	97.85	94.26	82.53	82.42	31.92
Personalization	PromptFL	96.93	96.92	85.05	87.97	60.27
	CoCoOp	95.31	96.11	81.80	88.98	66.67
	VPT	91.86	96.55	82.16	88.86	64.06
	FedAKT(C)	65.88	77.22	27.24	66.52	50.98
	FedGH(C)	40.68	63.31	1.97	55.62	5.33
	FedCLIP	81.12	96.14	80.28	84.41	40.14
	FedAVG	92.07	96.72	84.62	87.73	62.77
	FedOT	95.45	96.74	85.13	88.63	68.93
	FedOT(+B)	98.14	97.14	87.44	89.80	68.94
Comprehensive	PromptFL	96.88	96.34	84.11	86.39	55.13
	CoCoOp	74.60	94.34	79.88	80.40	57.90
	VPT	85.93	96.09	81.89	86.96	56.81
	FedAKT(C)	52.02	61.76	20.78	58.82	39.68
	FedGH(C)	39.99	61.18	1.91	52.76	6.79
	FedCLIP	80.86	95.76	80.25	83.66	38.44
	FedAVG	92.22	96.16	83.92	86.35	55.13
	FedOT	95.31	96.22	84.17	86.75	60.39
	FedOT(+B)	98.07	96.42	86.21	87.96	59.69

5.2 Results

Effectiveness of FedOT. As shown in Table 1, our proposed methods, FedOT and FedOT(+B), consistently outperform all baselines across the evaluation metrics, achieving strong generalization and personalization. Unlike methods such as FedAVG, FedCLIP, and PromptFL, which rely solely on global parameters, our approach incorporates local parameters, resulting in significantly better personalization while maintaining comparable or superior generalization performance. This demonstrates that combining global and local components is crucial for effective domain adaptation in federated settings, overcoming the limitations of purely global methods. On PACS, VPT shows the highest generalization accuracy—a result inconsistent with its performance on other datasets. Nevertheless, our method achieves the best personalization score and ultimately ranks highest in overall accuracy, reflecting robust and balanced performance. Even CoCoOp, FedGH, and FedAKT show modest gains or minimal drops in personalization, and fail to generalize to unseen domains, indicating poor robustness to distribution shifts, whereas ours not only achieves effective personalization but also demonstrates strong generalization to unseen domains. These results underscore the importance of balancing local adaptability and global knowledge integration, a balance that FedOT fulfills through its orthogonal transformations and globally shared classifier.

DOF and Personalization via FedOT(+B). Figure 2 illustrates how personalization performance varies with degrees of freedom (DOF) in block-diagonal orthogonal transformations (FedOT(+B)). Simpler tasks, such as FEMNIST, benefit from lower DOF due to preserved pretrained manifolds, whereas the complex OfficeHome dataset achieves better performance with higher DOF, capturing

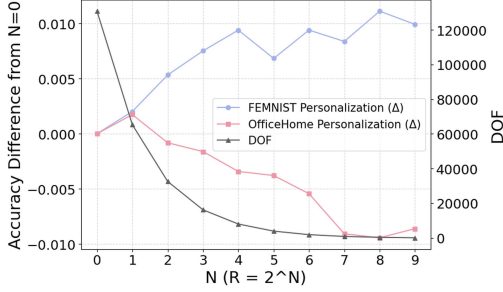


Figure 2: **Comparison of DOF and personalization accuracy on FEMNIST and OfficeHome.** We vary the number of blocks $R = 2^N$ in our block-diagonal transforms. The left axis depicts the change in personalization accuracy relative to $N = 0$ ($R = 1$), while the right axis shows the corresponding DOF values.

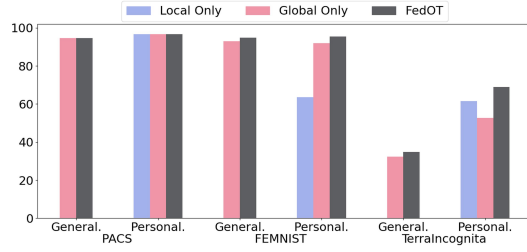


Figure 3: **Comparison of generalization and personalization performance for the local-only, global-only, and FedOT on FEMNIST, PACS, and TerraIncognita.** FedOT consistently outperforms both ablated methods, highlighting the complementary benefits of jointly leveraging local and global parameters.

richer patterns. This highlights the necessity of adjusting DOF according to dataset complexity, where block-orthogonality maintains parameter orthogonality and mitigates gradient conflicts, facilitating effective personalization in federated learning.

Condition Number and Generalization. Table 2 compares FedOT (with orthogonality constraint) and FedOT(-o) (without orthogonality constraint). Notably, FedOT preserves a low condition number ($\kappa = 1.0$) for all target clients and achieves high generalization accuracy. Imposing orthogonality keeps the transformation matrix well-conditioned and prevents over-scaling or distortion, thus maintaining robust generalization. By contrast, FedOT(-o) permits a steep rise in the condition number (κ up to 63.82), which severely impairs generalization performance. As implied by Theorem 4.1, larger κ magnifies gradient discrepancies across clients, undermining accuracy.

Table 2: **Comparison of generalization accuracy (%) and the final condition number κ .**

FEMNIST					PACS					Terra-Incognita				
Target	FedOT		FedOT(-o)		Target	FedOT		FedOT(-o)		Target	FedOT		FedOT(-o)	
	Acc.	κ	Acc.	κ		Acc.	κ	Acc.	κ		Acc.	κ	Acc.	κ
33	95.92%	1.00	59.18%	19.57	A	95.35%	1.00	95.35%	1.24	L38	44.34%	1.00	33.18%	1.37
0	96.15%	1.00	74.04%	43.45	C	97.44%	1.00	97.01%	1.30	L43	29.89%	1.00	31.51%	1.38
25	92.31%	1.00	67.31%	30.86	P	99.70%	1.00	99.70%	1.31	L46	42.19%	1.00	36.22%	1.34
26	95.19%	1.00	84.13%	35.15	S	86.24%	1.00	85.99%	1.12	L100	22.77%	1.00	21.74%	1.37
AVG	94.89%	1.00	71.17%	32.26	AVG	94.68%	1.00	94.51%	1.24	AVG	34.80%	1.00	30.66%	1.36

5.3 Ablation Study

Global and Local Parameters. To demonstrate the significance of incorporating both global and local parameters in our proposed method, we compare our approach on FEMNIST, PACS, and TerraIncognita with two ablated methods, one without global parameters and the other without local parameters. For generalization accuracy, we exclusively compare our method with the global-only method, as the local-only method is tied to domain-specific parameters, making it incompatible with the fundamental principles of FL settings. Referring to Figure 3, FedOT improves generalization across all datasets by incorporating local parameters, compared to the global-only approach. Additionally, our method surpasses both alternatives in personalization performance, highlighting that the joint utilization of global and local parameters provides significant advantages over relying solely on either. These results underscore the effectiveness of jointly integrating local and global parameters, indicating their complementary contribution to achieving superior performance in both personalization and generalization.

Towards Vision Foundation Models. To investigate the potential applicability of our framework to vision foundation models, we conduct experiments under the same settings as FedOT, but with a randomly initialized classifier. As shown in Table 3, despite the absence of explicit alignment

Table 3: **Accuracy results from experiments with different initialization methods for global parameters.** TextEnc uses the text encoder of CLIP for initialization, while RandInit uses random initialization.

	FEMNIST		PACS		OfficeHome		VLCS		TerraIncognita	
	TextEnc	RandInit	TextEnc	RandInit	TextEnc	RandInit	TextEnc	RandInit	TextEnc	RandInit
Generalization	94.89	96.15	94.68	90.91	81.30	82.67	81.11	76.12	34.80	27.20
Personalization	95.46	96.36	96.74	96.91	85.13	87.66	88.63	86.91	68.93	65.82
Comprehensive	95.31	96.31	96.22	95.41	84.17	86.42	86.75	84.21	60.39	56.17

between text and image representations, our framework demonstrates highly competitive performance when applied to foundation models composed solely of an image encoder. Notably, on FEMNIST and Office-Home, the randomly initialized method outperforms across all metrics, which suggests that datasets with weaker zero-shot capabilities and less aligned representations may benefit from learning alignment from scratch. These findings indicate that our approach maintains strong performance even without a pre-trained classifier, affirming that our framework can seamlessly integrate with any foundation model by leveraging only its image encoder.

Robustness to Communication Rounds. In an FL environment, where performance is profoundly influenced by the frequency of communication rounds between clients and the server, it is essential to assess the impact of varying communication intervals. To explore the effect of the local update epoch E in FL, we compare our method with FedCLIP while varying the number of local learning epochs to 1, 2, 4, and 8. As illustrated in Figure 4, our method consistently outperforms FedCLIP across all communication rounds and even exhibits performance improvement as the number of rounds increases. In contrast, FedCLIP tends to degrade in performance with more communication rounds, indicating its limitations for practical deployment. These results demonstrate the superiority of our method and its robustness for real-world FL applications.

Multi-Client Scenario. To assess the applicability of our method in a realistic FL environment, we consider a cross-device setting reflecting real-world conditions. Specifically, we set up 5 selected test clients and training clients of 2, 5, 10, and 15, using the FEMNIST dataset. The training environments for each client were kept consistent, as described in the implementation details. As depicted in Figure 5, the average generalization performance improvement of the test clients, compared to zero-shot model inference performance, was observed to be 12.62%, 22.36%, 26.40%, and 25.83%, respectively. These findings suggest that, despite the data heterogeneity among clients, an increase in the number of participating clients leads to a notable average performance enhancement when applying our framework in FL. Thus, our approach is also well-suited for cross-device FL contexts.

6 Limitations and Future Works

Although FedOT treats the foundation model as a black box to protect proprietary information, the use of a shared global classifier introduces some white-box elements. This can be restrictive when a strict black-box approach is mandatory. Future research may consider richer, nonlinear mappings—instead of strictly linear (orthogonal) ones—to better handle heterogeneous client data, despite reduced transparency in theoretical guarantees. Additionally, projecting data transformations into lower-dimensional spaces could improve computational efficiency on resource-constrained devices, though it may risk losing important semantic distinctions. This is because, while block-diagonal designs effectively decrease model complexity, determining optimal block sizes or tailoring them to individual clients remains challenging.

7 Conclusion

In this work, we proposed FedOT, a federated learning framework that integrates large-scale foundation models with orthogonal transformations to address both generalization and personalization. By leveraging a global classifier and local orthogonal transformations, our method mitigates gradient conflicts, preserves semantic information, and achieves consistent performance improvement on multiple datasets. The black-box nature introduced to the image encoder safeguards the intellectual property of the server and data privacy for clients, making FedOT a practical and effective solution for real-world federated applications that demand robust performance across highly diverse domains.

References

- [1] Josh Achiam, Steven Adler, Sandhini Agarwal, Lama Ahmad, Ilge Akkaya, Florencia Leoni Aleman, Diogo Almeida, Janko Altschmidt, Sam Altman, and Shyamal Anadkat. Gpt-4 technical report. *arXiv preprint arXiv:2303.08774*, 2023.
- [2] Rohan Anil, Andrew M Dai, Orhan Firat, Melvin Johnson, Dmitry Lepikhin, Alexandre Passos, Siamak Shakeri, Emanuel Taropa, Paige Bailey, and Zhifeng Chen. Palm 2 technical report. *arXiv preprint arXiv:2305.10403*, 2023.
- [3] Yogesh Balaji, Swami Sankaranarayanan, and Rama Chellappa. Metareg: Towards domain generalization using meta-regularization. *Advances in neural information processing systems*, 31, 2018.
- [4] Sara Beery, Grant Van Horn, and Pietro Perona. Recognition in terra incognita. In *Proceedings of the European conference on computer vision (ECCV)*, pages 456–473, 2018.
- [5] Rishi Bommasani, Drew A. Hudson, Ehsan Adeli, Russ Altman, Simran Arora, Sydney von Arx, Michael S. Bernstein, Jeannette Bohg, Antoine Bosselut, Emma Brunskill, Erik Brynjolfsson, S. Buch, Dallas Card, Rodrigo Castellon, Niladri S. Chatterji, Annie S. Chen, Kathleen A. Creel, Jared Davis, Dora Demszky, Chris Donahue, Moussa Doumbouya, Esin Durmus, Stefano Ermon, John Etchemendy, Kavin Ethayarajh, Li Fei-Fei, Chelsea Finn, Trevor Gale, Lauren E. Gillespie, Karan Goel, Noah D. Goodman, Shelby Grossman, Neel Guha, Tatsunori Hashimoto, Peter Henderson, John Hewitt, Daniel E. Ho, Jenny Hong, Kyle Hsu, Jing Huang, Thomas F. Icard, Saahil Jain, Dan Jurafsky, Pratyusha Kalluri, Siddharth Karamcheti, Geoff Keeling, Fereshte Khani, O. Khattab, Pang Wei Koh, Mark S. Krass, Ranjay Krishna, Rohith Kuditipudi, Ananya Kumar, Faisal Ladhak, Mina Lee, Tony Lee, Jure Leskovec, Isabelle Levent, Xiang Lisa Li, Xuechen Li, Tengyu Ma, Ali Malik, Christopher D. Manning, Suvir P. Mirchandani, Eric Mitchell, Zanele Munyikwa, Suraj Nair, Avanika Narayan, Deepak Narayanan, Benjamin Newman, Allen Nie, Juan Carlos Niebles, Hamed Nilforoshan, J. F. Nyarko, Giray Ogut, Laurel Orr, Isabel Papadimitriou, Joon Sung Park, Chris Piech, Eva Portelance, Christopher Potts, Aditi Raghunathan, Robert Reich, Hongyu Ren, Frieda Rong, Yusuf H. Roohani, Camilo Ruiz, Jack Ryan, Christopher R’e, Dorsa Sadigh, Shiori Sagawa, Keshav Santhanam, Andy Shih, Krishna Parasuram Srinivasan, Alex Tamkin, Rohan Taori, Armin W. Thomas, Florian Tramèr, Rose E. Wang, William Wang, Bohan Wu, Jiajun Wu, Yuhuai Wu, Sang Michael Xie, Michihiro Yasunaga, Jiaxuan You, Matei A. Zaharia, Michael Zhang, Tianyi Zhang, Xikun Zhang, Yuhui Zhang, Lucia Zheng, Kaitlyn Zhou, and Percy Liang. On the opportunities and risks of foundation models. *ArXiv*, 2021.
- [6] K. Bousmalis, G. Trigeorgis, N. Silberman, D. Krishnan, and D. Erhan. Domain separation networks. In *Advances in Neural Information Processing Systems 29 (NeurIPS)*, pages 343–351, Barcelona, Spain, 2016. Curran Associates, Inc.
- [7] Tom Brown, Benjamin Mann, Nick Ryder, Melanie Subbiah, Jared D Kaplan, Prafulla Dhariwal, Arvind Neelakantan, Pranav Shyam, Girish Sastry, and Amanda Askell. Language models are few-shot learners. *Advances in neural information processing systems*, 33:1877–1901, 2020.
- [8] Sebastian Caldas, Sai Meher Karthik Duddu, Peter Wu, Tian Li, Jakub Konečný, H Brendan McMahhan, Virginia Smith, and Ameet Talwalkar. Leaf: A benchmark for federated settings. *arXiv preprint arXiv:1812.01097*, 2018.
- [9] Amaia Cardiel et al. LLM-Wrapper: Black-box adaptation of VLMs for referring expression. In *International Conference on Learning Representations*, 2025.
- [10] Mathilde Caron, Hugo Touvron, Ishan Misra, Hervé Jégou, Julien Mairal, Piotr Bojanowski, and Armand Joulin. Emerging properties in self-supervised vision transformers. In *Proceedings of the IEEE/CVF international conference on computer vision*, pages 9650–9660, 2021.
- [11] Arthur Cayley. Sur quelques propriétés des déterminants gauches. 1846.
- [12] Annie S Chen, Yoonho Lee, Amrith Setlur, Sergey Levine, and Chelsea Finn. Project and probe: Sample-efficient domain adaptation by interpolating orthogonal features. *arXiv preprint arXiv:2302.05441*, 2023.
- [13] L. Chen, Y. Zhang, Y. Song, Y. Shan, and L. Liu. Improved test-time adaptation for domain generalization. In *Proceedings of the IEEE/CVF Conference on Computer Vision and Pattern Recognition (CVPR)*, pages 24172–24182, 2023.
- [14] Xinlei Chen and Kaiming He. Exploring simple siamese representation learning. In *Proceedings of the IEEE/CVF conference on computer vision and pattern recognition*, pages 15750–15758, 2021.

- [15] Xinlei Chen, Saining Xie, and Kaiming He. An empirical study of training self-supervised vision transformers. In *Proceedings of the IEEE/CVF international conference on computer vision*, pages 9640–9649, 2021.
- [16] Yiqiang Chen, Wang Lu, Xin Qin, Jindong Wang, and Xing Xie. MetaFed: Federated learning among federations with cyclic knowledge distillation for personalized healthcare. *IEEE Transactions on Neural Networks and Learning Systems*, 2023.
- [17] Wonguk Cho, Jinha Park, and Taesup Kim. Complementary domain adaptation and generalization for unsupervised continual domain shift learning. *arXiv preprint arXiv:2303.15833*, 2023.
- [18] Myung Jin Choi, Joseph J Lim, Antonio Torralba, and Alan S Willsky. Exploiting hierarchical context on a large database of object categories. In *2010 IEEE computer society conference on computer vision and pattern recognition*, pages 129–136. IEEE, 2010.
- [19] Aakanksha Chowdhery, Sharan Narang, Jacob Devlin, Maarten Bosma, Gaurav Mishra, Adam Roberts, Paul Barham, Hyung Won Chung, Charles Sutton, and Sebastian Gehrmann. Palm: Scaling language modeling with pathways. *Journal of Machine Learning Research*, 24(240):1–113, 2023.
- [20] Gregory Cohen, Saeed Afshar, Jonathan Tapson, and Andre Van Schaik. Emnist: Extending mnist to handwritten letters. In *2017 international joint conference on neural networks (IJCNN)*, pages 2921–2926. IEEE, 2017.
- [21] Jacob Devlin, Ming-Wei Chang, Kenton Lee, and Kristina Toutanova. Bert: Pre-training of deep bidirectional transformers for language understanding. *arXiv preprint arXiv:1810.04805*, 2018.
- [22] Mark Everingham, Luc Van Gool, Christopher KI Williams, John Winn, and Andrew Zisserman. The pascal visual object classes (voc) challenge. *International journal of computer vision*, 88:303–338, 2010.
- [23] Chen Fang, Ye Xu, and Daniel N Rockmore. Unbiased metric learning: On the utilization of multiple datasets and web images for softening bias. In *Proceedings of the IEEE International Conference on Computer Vision*, pages 1657–1664, 2013.
- [24] Abolfazl Farahani, Sahar Voghoei, Khaled Rasheed, and Hamid R Arabnia. A brief review of domain adaptation. *Advances in data science and information engineering*, pages 877–894, 2021.
- [25] Li Fei-Fei, Rob Fergus, and Pietro Perona. Learning generative visual models from few training examples: An incremental bayesian approach tested on 101 object categories. In *2004 conference on computer vision and pattern recognition workshop*, pages 178–178. IEEE, 2004.
- [26] Yaroslav Ganin and Victor Lempitsky. Unsupervised domain adaptation by backpropagation. In *International conference on machine learning*, pages 1180–1189. PMLR, 2015.
- [27] Dashan Gao, Xin Yao, and Qiang Yang. A survey on heterogeneous federated learning. *arXiv preprint arXiv:2210.04505*, 2022.
- [28] Muhammad Ghifary, W Bastiaan Kleijn, Mengjie Zhang, David Balduzzi, and Wen Li. Deep reconstruction-classification networks for unsupervised domain adaptation. In *Computer Vision—ECCV 2016: 14th European Conference, Amsterdam, The Netherlands, October 11–14, 2016, Proceedings, Part IV 14*, pages 597–613. Springer, 2016.
- [29] S. Gong, C. Cui, C. Zhang, W. Wang, X. Nie, and L. Zhu. Federated domain generalization via prompt learning and aggregation (plan). *arXiv:2411.10063*, 2024.
- [30] Xuan Gong, Abhishek Sharma, Srikrishna Karanam, Ziyan Wu, Terrence Chen, David Doermann, and Arun Innanje. Preserving privacy in federated learning with ensemble cross-domain knowledge distillation. In *Proceedings of the AAAI Conference on Artificial Intelligence*, volume 36, pages 11891–11899, 2022.
- [31] Jean-Bastien Grill, Florian Strub, Florent Altché, Corentin Tallec, Pierre Richemond, Elena Buchatskaya, Carl Doersch, Bernardo Avila Pires, Zhaohan Guo, and Mohammad Gheshlaghi Azar. Bootstrap your own latent—a new approach to self-supervised learning. *Advances in neural information processing systems*, 33:21271–21284, 2020.
- [32] Ishaan Gulrajani and David Lopez-Paz. In search of lost domain generalization. *arXiv preprint arXiv:2007.01434*, 2020.
- [33] Tao Guo, Song Guo, Junxiao Wang, Xueyang Tang, and Wenchao Xu. Promptfl: Let federated participants cooperatively learn prompts instead of models—federated learning in age of foundation model. *IEEE Transactions on Mobile Computing*, 23(5):5179–5194, 2023.

- [34] Zixian Guo, Yuxiang Wei, Ming Liu, Zhilong Ji, Jinfeng Bai, Yiwen Guo, and Wangmeng Zuo. Black-box tuning of vision-language models with effective gradient approximation. *arXiv preprint arXiv:2312.15901*, 2024.
- [35] Kaiming He, Haoqi Fan, Yuxin Wu, Saining Xie, and Ross Girshick. Momentum contrast for unsupervised visual representation learning. In *Proceedings of the IEEE/CVF conference on computer vision and pattern recognition*, pages 9729–9738, 2020.
- [36] Edward J Hu, Yelong Shen, Phillip Wallis, Zeyuan Allen-Zhu, Yuanzhi Li, Shean Wang, Lu Wang, and Weizhu Chen. Lora: Low-rank adaptation of large language models. *arXiv preprint arXiv:2106.09685*, 2021.
- [37] Chao Jia, Yinfei Yang, Ye Xia, Yi-Ting Chen, Zarana Parekh, Hieu Pham, Quoc Le, Yun-Hsuan Sung, Zhen Li, and Tom Duerig. Scaling up visual and vision-language representation learning with noisy text supervision. In *International conference on machine learning*, pages 4904–4916. PMLR, 2021.
- [38] Menglin Jia, Luming Tang, Bor-Chun Chen, Claire Cardie, Serge Belongie, Bharath Hariharan, and Ser-Nam Lim. Visual prompt tuning. In *European Conference on Computer Vision*, pages 709–727. Springer, 2022.
- [39] Jakub Konečný, H Brendan McMahan, Daniel Ramage, and Peter Richtárik. Federated optimization: Distributed machine learning for on-device intelligence. *arXiv preprint arXiv:1610.02527*, 2016.
- [40] Jakub Konečný, H Brendan McMahan, Felix X Yu, Peter Richtárik, Ananda Theertha Suresh, and Dave Bacon. Federated learning: Strategies for improving communication efficiency. *arXiv preprint arXiv:1610.05492*, 2016.
- [41] Ang Li, Jingwei Sun, Xiao Zeng, Mi Zhang, Hai Li, and Yiran Chen. Fedmask: Joint computation and communication-efficient personalized federated learning via heterogeneous masking. In *Proceedings of the 19th ACM Conference on Embedded Networked Sensor Systems*, pages 42–55, 2021.
- [42] Da Li, Yongxin Yang, Yi-Zhe Song, and Timothy M Hospedales. Deeper, broader and artier domain generalization. In *Proceedings of the IEEE international conference on computer vision*, pages 5542–5550, 2017.
- [43] Da Li, Jianshu Zhang, Yongxin Yang, Cong Liu, Yi-Zhe Song, and Timothy M Hospedales. Episodic training for domain generalization. In *Proceedings of the IEEE/CVF International Conference on Computer Vision*, pages 1446–1455, 2019.
- [44] Daliang Li and Junpu Wang. Fedmd: Heterogenous federated learning via model distillation. *arXiv preprint arXiv:1910.03581*, 2019.
- [45] Shichong Liu, Haozhe Jin, Zhiwei Tang, Rui Zhai, Ke Lu, Junyang Yu, and Chenxi Bai. Adapter-guided knowledge transfer for heterogeneous federated learning. *Journal of Systems Architecture*, 159:103338, 2025.
- [46] Weiyang Liu, Zeju Qiu, Yao Feng, Yuliang Xiu, Yuxuan Xue, Longhui Yu, Haiwen Feng, Zhen Liu, Juyeon Heo, and Songyou Peng. Parameter-efficient orthogonal finetuning via butterfly factorization. *arXiv preprint arXiv:2311.06243*, 2023.
- [47] Mingsheng Long, Yue Cao, Jianmin Wang, and Michael Jordan. Learning transferable features with deep adaptation networks. In *International conference on machine learning*, pages 97–105. PMLR, 2015.
- [48] Wang Lu, Xixu Hu, Jindong Wang, and Xing Xie. Fedclip: Fast generalization and personalization for clip in federated learning. *arXiv preprint arXiv:2302.13485*, 2023.
- [49] Wang Lu, Jindong Wang, Yiqiang Chen, Xin Qin, Renjun Xu, Dimitrios Dimitriadis, and Tao Qin. Personalized federated learning with adaptive batchnorm for healthcare. *IEEE Transactions on Big Data*, 2022.
- [50] Wang Lu, Hao Yu, Jindong Wang, Damien Teney, Haohan Wang, Yao Zhu, Yiqiang Chen, Qiang Yang, Xing Xie, and Xiangyang Ji. Zoopfl: Exploring black-box foundation models for personalized federated learning. In *International Workshop on Trustworthy Federated Learning*, pages 19–35. Springer, 2024.
- [51] Brendan McMahan, Eider Moore, Daniel Ramage, Seth Hampson, and Blaise Agüera y Arcas. Communication-efficient learning of deep networks from decentralized data. In *Artificial intelligence and statistics*, pages 1273–1282. PMLR, 2017.

- [52] Fan'an Meng, Cheng Cui, Hao Dai, and Shaogang Gong. Black-box test-time prompt tuning for vision-language models. In *Proceedings of the AAAI Conference on Artificial Intelligence*, volume 39, pages 6099–6107, 2025.
- [53] Krikamol Muandet, David Balduzzi, and Bernhard Schölkopf. Domain generalization via invariant feature representation. In *International conference on machine learning*, pages 10–18. PMLR, 2013.
- [54] A Tuan Nguyen, Toan Tran, Yarin Gal, and Atilim Gunes Baydin. Domain invariant representation learning with domain density transformations. *Advances in Neural Information Processing Systems*, 34:5264–5275, 2021.
- [55] J. Niemeijer, M. Schwonberg, J.-A. Termöhlen, N. M. Schmidt, and T. Fingscheidt. Generalization by adaptation: Diffusion-based domain extension for domain-generalized semantic segmentation. In *Proceedings of the IEEE/CVF Winter Conference on Applications of Computer Vision (WACV)*, pages 2830–2840, 2024.
- [56] Changdae Oh, Hyeji Hwang, Hee-young Lee, YongTaek Lim, Geunyoung Jung, Jiyoung Jung, Hosik Choi, and Kyungwoo Song. BlackVIP: Black-box visual prompting for robust transfer learning. In *Proceedings of the IEEE/CVF Conference on Computer Vision and Pattern Recognition*, 2023.
- [57] Aitor Ormazabal, Mikel Artetxe, and Eneko Agirre. CombLM: Adapting black-box language models through small fine-tuned models. In *Proceedings of the 2023 Conference on Empirical Methods in Natural Language Processing*, pages 2961–2974, Singapore, 2023.
- [58] Yassine Ouali, Adrian Bulat, Brais Martinez, and Georgios Tzimiropoulos. Black box few-shot adaptation for vision-language models. In *Proceedings of the IEEE/CVF International Conference on Computer Vision*, 2023.
- [59] Jay N. Paranjape, Shameema Sikder, S. Swaroop Vedula, and Vishal M. Patel. Blackbox adaptation for medical image segmentation. In *Proceedings of the International Conference on Medical Image Computing and Computer-Assisted Intervention (MICCAI)*, 2024.
- [60] Jay N. Paranjape, Shameema Sikder, S. Swaroop Vedula, and Vishal M. Patel. Federated black-box adaptation for semantic segmentation. In *Proceedings of the 38th Conference on Neural Information Processing Systems (NeurIPS)*, 2024.
- [61] Adam Paszke, Sam Gross, Francisco Massa, Adam Lerer, James Bradbury, Gregory Chanan, Trevor Killeen, Zeming Lin, Natalia Gimelshein, and Luca Antiga. Pytorch: An imperative style, high-performance deep learning library. In *Advances in neural information processing systems*, pages 8026–8037, 2019.
- [62] Zhongyi Pei, Zhangjie Cao, Mingsheng Long, and Jianmin Wang. Multi-adversarial domain adaptation. In *Proceedings of the AAAI conference on artificial intelligence*, volume 32, 2018.
- [63] Krishna Pillutla, Kshitiz Malik, Abdel-Rahman Mohamed, Mike Rabbat, Maziar Sanjabi, and Lin Xiao. Federated learning with partial model personalization. In *International Conference on Machine Learning*, pages 17716–17758. PMLR, 2022.
- [64] Zeju Qiu, Weiyang Liu, Haiwen Feng, Yuxuan Xue, Yao Feng, Zhen Liu, Dan Zhang, Adrian Weller, and Bernhard Schölkopf. Controlling text-to-image diffusion by orthogonal finetuning. *Advances in Neural Information Processing Systems*, 36, 2024.
- [65] Alec Radford, Jong Wook Kim, Chris Hallacy, Aditya Ramesh, Gabriel Goh, Sandhini Agarwal, Girish Sastry, Amanda Askell, Pamela Mishkin, Jack Clark, et al. Learning transferable visual models from natural language supervision. In *International conference on machine learning*, pages 8748–8763. PMLR, 2021.
- [66] Alec Radford, Jeffrey Wu, Rewon Child, David Luan, Dario Amodei, and Ilya Sutskever. Language models are unsupervised multitask learners. *OpenAI blog*, 1(8):9, 2019.
- [67] Bryan C Russell, Antonio Torralba, Kevin P Murphy, and William T Freeman. Labelme: a database and web-based tool for image annotation. *International journal of computer vision*, 77:157–173, 2008.
- [68] Shiv Shankar, Vihari Piratla, Soumen Chakrabarti, Siddhartha Chaudhuri, Preethi Jyothi, and Sunita Sarawagi. Generalizing across domains via cross-gradient training. *arXiv preprint arXiv:1804.10745*, 2018.
- [69] Karan Singhal, Hakim Sidahmed, Zachary Garrett, Shanshan Wu, John Rush, and Sushant Prakash. Federated reconstruction: Partially local federated learning. *Advances in Neural Information Processing Systems*, 34:11220–11232, 2021.

- [70] B. Sun and K. Saenko. Deep coral: Correlation alignment for deep domain adaptation. In *Proceedings of the European Conference on Computer Vision (ECCV) Workshops*, pages 443–450, Amsterdam, The Netherlands, 2016. Springer.
- [71] Tianxiang Sun, Yunfan Shao, Hong Qian, Xuanjing Huang, and Xipeng Qiu. Black-box tuning for language-model-as-a-service. In *Proceedings of the 39th International Conference on Machine Learning*, volume 162, 2022.
- [72] Hugo Touvron, Thibaut Lavril, Gautier Izacard, Xavier Martinet, Marie-Anne Lachaux, Timothée Lacroix, Baptiste Rozière, Naman Goyal, Eric Hambro, and Faisal Azhar. Llama: Open and efficient foundation language models. *arXiv preprint arXiv:2302.13971*, 2023.
- [73] Eric Tzeng, Judy Hoffman, Trevor Darrell, and Kate Saenko. Simultaneous deep transfer across domains and tasks. In *Proceedings of the IEEE international conference on computer vision*, pages 4068–4076, 2015.
- [74] Hemanth Venkateswara, Jose Eusebio, Shayok Chakraborty, and Sethuraman Panchanathan. Deep hashing network for unsupervised domain adaptation. In *Proceedings of the IEEE conference on computer vision and pattern recognition*, pages 5018–5027, 2017.
- [75] Guoyizhe Wei, Feng Wang, Anshul Shah, and Rama Chellappa. Dual prompt tuning for domain-aware federated learning. *arXiv preprint arXiv:2310.03103*, 2023.
- [76] Jinze Wu, Qi Liu, Zhenya Huang, Yuting Ning, Hao Wang, Enhong Chen, Jinfeng Yi, and Bowen Zhou. Hierarchical personalized federated learning for user modeling. In *Proceedings of the Web Conference 2021*, pages 957–968, 2021.
- [77] Guangxuan Xiao, Ji Lin, and Song Han. Offsite-tuning: Transfer learning without full model. *arXiv preprint arXiv:2302.04870*, 2023.
- [78] Ting Yao, Yingwei Pan, Chong-Wah Ngo, Houqiang Li, and Tao Mei. Semi-supervised domain adaptation with subspace learning for visual recognition. In *Proceedings of the IEEE conference on Computer Vision and Pattern Recognition*, pages 2142–2150, 2015.
- [79] Liping Yi, Gang Wang, Xiaoguang Liu, Zhuan Shi, and Han Yu. Fedgh: Heterogeneous federated learning with generalized global header. In *Proceedings of the 31st ACM International Conference on Multimedia*, pages 8686–8696, 2023.
- [80] Lang Yu, Qin Chen, Jiaju Lin, and Liang He. Black-box prompt tuning for vision-language model as a service. In *Proceedings of the Thirty-Second International Joint Conference on Artificial Intelligence*, pages 1686–1694, 2023.
- [81] Jie Zhang, Song Guo, Xiaosong Ma, Haozhao Wang, Wenchao Xu, and Feijie Wu. Parameterized knowledge transfer for personalized federated learning. *Advances in Neural Information Processing Systems*, 34:10092–10104, 2021.
- [82] R. Zhang, Q. Xu, J. Yao, Y. Zhang, Q. Tian, and Y. Wang. Federated domain generalization with generalization adjustment. In *Proceedings of the IEEE/CVF Conference on Computer Vision and Pattern Recognition (CVPR)*, pages 3954–3963, 2023.
- [83] Renrui Zhang, Wei Zhang, Rongyao Fang, Peng Gao, Kunchang Li, Jifeng Dai, Yu Qiao, and Hongsheng Li. Tip-adapter: Training-free adaption of CLIP for few-shot classification. In *Computer Vision – ECCV 2022*, pages 493–510, 2022.
- [84] Kaiyang Zhou, Jingkang Yang, Chen Change Loy, and Ziwei Liu. Conditional prompt learning for vision-language models. In *Proceedings of the IEEE/CVF conference on computer vision and pattern recognition*, pages 16816–16825, 2022.
- [85] Kaiyang Zhou, Jingkang Yang, Chen Change Loy, and Ziwei Liu. Learning to prompt for vision-language models. *International Journal of Computer Vision*, 130(9):2337–2348, 2022.

Appendix

A Related Work

A.1 Foundation Models

Foundation models [5], exemplified by the GPT series [66, 7, 1], vision-language models (VLMs)[65, 37], and others[21, 19, 2, 72], represent a transformative phase in artificial intelligence. These models are characterized by their unprecedented scale, extensive pre-training, and remarkable performance across a wide range of downstream tasks.

Notably, the success of contrastive pre-training in visual tasks [35, 31, 10, 14, 15] has driven the adoption of multi-modal contrastive pre-training as a core strategy in contemporary research. CLIP [65] serves as a representative example of this trend, showcasing the potential of aligning visual and language modalities for diverse applications. In this study, we focus on vision foundation models, including VLMs such as CLIP, and highlight their potential for extension to federated learning in vision tasks.

A.2 Federated Learning

Federated Learning (FL) is a machine learning approach that enables model training across multiple devices or servers holding local data without requiring data centralization [39, 40, 51]. This framework offers significant advantages, particularly in preserving data privacy and efficiently utilizing resources, as it eliminates the need to transmit large volumes of sensitive data to a central server. FL is generally categorized into homogeneous and heterogeneous paradigms. Homogeneous FL assumes similar computational power and data distribution across all clients, allowing for a uniform training process. In contrast, heterogeneous FL involves clients with diverse computational resources and non-IID (independent and identically distributed) data, presenting substantial challenges in training and model aggregation [27]. Designing systems that can effectively address such client diversity is crucial. To this end, personalized FL—an approach that trains personalized local models alongside a global model—has emerged as a key strategy to handle model heterogeneity [63, 69, 44, 81, 30, 41]. The advent of large-scale pre-trained VLMs, such as CLIP [65], has further driven research in FL, encouraging exploration into the integration of VLMs within the FL framework [48, 33, 75].

B Preliminaries

B.1 Contrastive Language-Image Pretraining (CLIP)

A pre-trained CLIP model architecture features a dual-stream design, comprising a text encoder, denoted as \mathcal{T}_ϕ , and an image encoder, \mathcal{I}_θ , where ϕ and θ represent the pre-trained parameters. For a given task τ with a set of classes $Y^\tau = \{y_c^\tau\}_{c=1}^{K^\tau}$, where K^τ denotes the number of classes for classification, the model utilizes a set of class embeddings $t^\tau = \{\mathcal{T}_\phi(p_c^\tau)\}_{c=1}^{K^\tau}$. These embeddings are generated through natural language prompting $p_c^\tau = \text{"a picture of a \{class name of } y_c^\tau \text{"}$. Upon receiving image data x , the corresponding embedding $\mathcal{I}_\theta(x)$ is matched against the class embeddings using cosine similarity $\text{Sim}(\cdot, \cdot)$, and the task-specific classification probability is then calculated as:

$$p(y = y_c^\tau | x; \phi, \theta, \tau) = \frac{e^{\alpha \cdot \text{Sim}(\mathcal{I}_\theta(x), \mathcal{T}_\phi(p_c^\tau))}}{\sum_{c'=1}^{C^\tau} e^{\alpha \cdot \text{Sim}(\mathcal{I}_\theta(x), \mathcal{T}_\phi(p_{c'}^\tau))}}$$

where α is a learnable scaling parameter, often described as the inverse of temperature. This procedure allows the set of class embeddings t^τ to act as a linear classifier.

B.2 Federated Learning Setting

In the conventional FL setting, N distinct clients collaborate to train a shared model. Each client, denoted as $i \in 1, 2, \dots, N$, is characterized by its unique data distribution $p^{(i)}(x, y)$. Each client i holds its own dataset $D^{(i)}$, comprising $M^{(i)}$ data points: $\{(x_k^{(i)}, y_k^{(i)})\}_{k=1}^{M^{(i)}}$. It is important to note that the data distribution $p^{(i)}(x, y)$ varies significantly across the clients, which are also interchangeably

referred to as domains. The primary goal within FL is the collaborative training of a shared model, parameterized by w , where the loss function for a specific data point (x, y) is defined as $\ell(w; x, y)$. The global objective function, which the collaborative effort seeks to minimize, is given by:

$$f(w) := \frac{1}{N} \sum_{i=1}^N f^{(i)}(w)$$

where $f^{(i)}(w)$ represents the local objective function for each client i , and it is defined as $f^{(i)}(w) = \mathbb{E}_{p^{(i)}(x, y)}[\ell(w; x, y)]$.

In this paper, we implement the FedAvg approach [51], a widely adopted federated averaging algorithm, as our base framework to train our global (shared) parameters in our proposed framework.

C FedOT

C.1 Detailed of Parameter Update.

The algorithm of FedOT is presented in the form of a complete pseudo-code.

Algorithm 1 FedOT: Orthogonal Local Updates via Cayley Transform

Global initialisation

- 1: Initialise server parameter $w_{g,0}$
- 2: **for all** client $i \in \{1, \dots, N\}$ **in parallel do**
- 3: $X_0^{(i)} \leftarrow I$
- 4: $P_0^{(i)} \leftarrow \frac{1}{2}(X_0^{(i)} - X_0^{(i)\top})$
- 5: $w_{1,0}^{(i)} \leftarrow (I + P_0^{(i)})(I - P_0^{(i)})^{-1}$
- 6: **end for**
- 7: Server broadcasts $w_{g,0}$ to all clients
- 8: **for** round $t = 0$ **to** $T - 1$ **do**
- 9: **for all** client i **in parallel do**
- 10: $(w_{g,t+1}^{(i)}, X_{t+1}^{(i)}) \leftarrow \text{LOCALUPDATE}(i, w_{g,t}, X_t^{(i)})$
- 11: Client sends $w_{g,t+1}^{(i)}$ to server
- 12: **end for**
- 13: **Server aggregation**
- 14: $w_{g,t+1} \leftarrow \frac{1}{N} \sum_{i=1}^N w_{g,t+1}^{(i)}$
- 15: Server broadcasts $w_{g,t+1}$ to all clients
- 16: **end for**
- 17: **function** LOCALUPDATE($i, w_g, X^{(i)}$)
- 18: $P^{(i)} \leftarrow \frac{1}{2}(X^{(i)} - X^{(i)\top})$
- 19: $w_1^{(i)} \leftarrow (I + P^{(i)})(I - P^{(i)})^{-1}$
- 20: **for** epoch $e = 1$ **to** E **do**
- 21: **for all** mini-batch $B \subset D^{(i)}$ **do**
- 22: $w_g^{(i)} \leftarrow w_g^{(i)} - \eta \nabla_{w_g^{(i)}} \ell^{(i)}(w_g^{(i)}, w_1^{(i)}; B)$
- 23: $X^{(i)} \leftarrow X^{(i)} - \eta \nabla_{X^{(i)}} \ell^{(i)}(w_g^{(i)}, w_1^{(i)}; B)$
- 24: $P^{(i)} \leftarrow \frac{1}{2}(X^{(i)} - X^{(i)\top})$
- 25: $w_1^{(i)} \leftarrow (I + P^{(i)})(I - P^{(i)})^{-1}$ ▷ Cayley transform
- 26: **end for**
- 27: **end for**
- 28: **return** $(w_g^{(i)}, X^{(i)})$ ▷ Only $w_g^{(i)}$ sent to server
- 29: **end function**

In this pseudo-code, each client i maintains an unconstrained matrix $X^{(i)}$, from which $w_1^{(i)}$ is derived via the Cayley transform. The function $P^{(i)} = \frac{1}{2}(X^{(i)} - (X^{(i)})^\top)$ ensures $P^{(i)}$ is skew-symmetric, so $(I - P^{(i)})$ remains invertible. After computing local updates, clients only send their updated

global parameters $w_g^{(i)}$ back to the server; $X^{(i)}$ and $w_1^{(i)}$ remain local. The server then aggregates the global parameters and broadcasts the new global parameter w_g to all clients, thus completing one communication round.

C.2 Cayley Transform

In mathematics, the Cayley transform, introduced by Arthur Cayley [11], maps skew-symmetric matrices to special orthogonal matrices. It is also used in real, complex, and quaternionic analysis. To integrate orthogonal transformations into our framework, we employ the Cayley transform and obtain orthogonal matrices corresponding to each client’s local parameters.

The process of the Cayley Transform. Given the original feature representations $z \in \mathbb{R}^d$ and an orthogonal matrix denoted $Q \in \mathbb{R}^{d \times d}$, the resulting orthogonally transformed features are denoted as $z' \in \mathbb{R}^d$. Thus, the transformation is expressed as $z' = Q \cdot z$, where $Q \cdot Q^\top = Q^\top \cdot Q = I$, underscoring the orthogonality of Q . To ensure orthogonal weight matrices during fine-tuning, we utilize the *Cayley transform*, enforcing orthogonality. In particular, the orthogonal matrix Q is derived using the equation $Q = (I + P)(I - P)^{-1}$, subject to the condition that $P = -P^\top$. To satisfy the constraint on P , we formulate P as $P = 0.5(X - X^\top)$, where X is a given transformation matrix.

Differentiability of the Cayley Transform. Because $P^{(i)}$ is skew-symmetric, $(I - P^{(i)})$ is guaranteed to be invertible (its eigenvalues cannot be 1). Thus, the Cayley transform $(I + P^{(i)})(I - P^{(i)})^{-1}$ is well-defined and differentiable. In this way, standard optimizers can be applied to $X^{(i)}$, and each forward/backward pass enforces the orthogonality of $w_1^{(i)}$ while preserving smooth gradients for end-to-end training.

D Comparison of Learning Frameworks

To further clarify our statements in 3.4, we compare different learning frameworks, with axis of data privacy, model ownership, computational efficiency, and their possible use cases. We refer to BlackFed [60] for the definition of Black-box FL, and refer to ZooPFL [50] for the definition of Black-box Foundation FL. Our method adopts Black-box Foundation FL, preserving proprietary foundation models.

Table 4: Comparison of learning frameworks and their applications.

Framework		Data Privacy	Model Ownership	Computational Efficiency	Use Case
White-box Learning	Traditional Learning	✓	✗	↓	Full fine-tuning on private GPU clusters (e.g., academic, enterprise internal data training)
	Federated Learning	✓	✗	↓	Edge-IoT with private data (e.g., smartphone keyboards, wearables, medical video collaboration)
Black-box Learning	Black-box TL	✗	✓	↑	Cloud AI API-based SaaS (e.g., GPT-4 chatbot, document summarization)
	Black-box FL	✓	✓	↓	On-device personalization (e.g., automotive, smart home, regulated on-site black-box servers)
	Black-box Foundation FL (Ours)	✓	✓	↑	

E Theoretical Analysis

E.1 Gradient Analysis with a Linear $w_1^{(i)}$

We begin by defining the cross-entropy loss for client i in a concise manner:

$$\ell^{(i)} = \mathbb{E}_{(x,y) \in D^{(i)}} [\text{CE}(r_x^{(i)}, y)],$$

where

$$r_x^{(i)} = \text{softmax}\left(\tau w_g^{(i)} \frac{w_1^{(i)} \mathcal{I}(x)}{\|w_1^{(i)} \mathcal{I}(x)\|}\right).$$

Here, $\mathcal{I}(\cdot)$ is the (frozen) vision encoder, $w_g^{(i)} \in \mathbb{R}^{K \times d}$ is the global classifier for client i , and $w_1^{(i)} \in \mathbb{R}^{d \times d}$ is the local linear transformation. A standard derivative computation gives

$$\nabla_{w_g^{(i)}} \ell^{(i)} = \mathbb{E}_{(x,y) \in D^{(i)}} \left[\tau (r_x^{(i)} - y) \left(\frac{w_1^{(i)} \mathcal{I}(x)}{\|w_1^{(i)} \mathcal{I}(x)\|} \right)^\top \right].$$

Linear Transformation Assumption. We identify $w_1^{(i)}$ as the client-specific linear map in $\mathbb{R}^{d \times d}$. Then,

$$\mathcal{I}'^{(i)}(x) = w_1^{(i)} \mathcal{I}(x).$$

Define

$$\Delta_i := r_x^{(i)} - y, \quad \|\Delta_i\| \leq 2 \quad (\text{since } \|r_x^{(i)}\| \leq 1 \text{ and } \|y\| \leq 1).$$

Substituting these into $\nabla_{w_g^{(i)}} \ell^{(i)}$:

$$\nabla_{w_g^{(i)}} \ell^{(i)} = \mathbb{E}_{(x,y) \in D^{(i)}} \left[\tau \Delta_i \left(\frac{w_1^{(i)} \mathcal{I}(x)}{\|w_1^{(i)} \mathcal{I}(x)\|} \right)^\top \right]. \quad (1)$$

E.2 Bounding the Gradient Difference

For clients i and j , the difference between their global-classifier gradients is

$$\left\| \nabla_{w_g^{(i)}} \ell^{(i)} - \nabla_{w_g^{(j)}} \ell^{(j)} \right\|.$$

Following similar derivations for each side, we obtain:

$$\begin{aligned} & \left\| \nabla_{w_g^{(i)}} \ell^{(i)} - \nabla_{w_g^{(j)}} \ell^{(j)} \right\|_2 \\ & \leq \mathbb{E}_{D^{(i)}} \left\| \tau \Delta_i \frac{w_1^{(i)} \mathcal{I}(x)}{\|w_1^{(i)} \mathcal{I}(x)\|} \right\| + \mathbb{E}_{D^{(j)}} \left\| \tau \Delta_j \frac{w_1^{(j)} \mathcal{I}(x)}{\|w_1^{(j)} \mathcal{I}(x)\|} \right\| \\ & \leq \mathbb{E}_{D^{(i)}} \left\| 2\tau \frac{w_1^{(i)} \mathcal{I}(x)}{\|w_1^{(i)} \mathcal{I}(x)\|} \right\| + \mathbb{E}_{D^{(j)}} \left\| 2\tau \frac{w_1^{(j)} \mathcal{I}(x)}{\|w_1^{(j)} \mathcal{I}(x)\|} \right\|, \end{aligned} \quad (2)$$

which, by noting that

$$\frac{\|w_1^{(i)} \mathcal{I}(x)\|}{\|w_1^{(i)} \mathcal{I}(x)\|} \leq \kappa(w_1^{(i)}),$$

leads to

$$\left\| \nabla_{w_g^{(i)}} \ell^{(i)} - \nabla_{w_g^{(j)}} \ell^{(j)} \right\| \leq 2\tau \left[\kappa(w_1^{(i)}) + \kappa(w_1^{(j)}) \right]. \quad (3)$$

E.3 Generalizing to Prompt Learning with $\mathbf{p}^{(i)}$

The preceding analysis treats $w_g^{(i)}$ as a directly learnable classifier. In a prompt-learning setting, however, the actual trainable quantity is a *prompt embedding* $\mathbf{p}^{(i)}$, which indirectly determines $w_g^{(i)}$. Concretely, suppose we have a learnable $\mathbf{p}^{(i)} \in \mathbb{R}^{K \times e}$ (e.g. K prompt tokens, each of dimension e), and a function

$$w_g^{(i)} = \mathcal{T}_\phi(\mathbf{p}^{(i)}),$$

where ϕ is the frozen text-encoder parameter, and \mathcal{T}_ϕ outputs a final text-embedding matrix in $\mathbb{R}^{K \times d}$. Adopting the same temperature τ and local transform $w_1^{(i)}$, the logits become

$$r_x^{(i)} = \text{softmax}\left(\tau \mathcal{T}_\phi(\mathbf{p}^{(i)}) \frac{w_1^{(i)} \mathcal{I}(x)}{\|w_1^{(i)} \mathcal{I}(x)\|}\right).$$

Thus, the cross-entropy loss for client i retains the same form:

$$\ell^{(i)} = \mathbb{E}_{(x,y) \in D^{(i)}} [\text{CE}(r_x^{(i)}, y)].$$

E.3.1 Gradient via Chain Rule

By the same derivation as Eq. (1), we have

$$\nabla_{w_g^{(i)}} \ell^{(i)} = \mathbb{E} \left[\tau \left(r_x^{(i)} - y \right) \left(\frac{w_1^{(i)} \mathcal{I}(x)}{\|w_1^{(i)} \mathcal{I}(x)\|} \right)^\top \right].$$

Since $w_g^{(i)} = \mathcal{T}_\phi(\mathbf{p}^{(i)})$, a standard chain rule yields

$$\nabla_{\mathbf{p}^{(i)}} \ell^{(i)} = \left(\frac{\partial w_g^{(i)}}{\partial \mathbf{p}^{(i)}} \right)^\top \nabla_{w_g^{(i)}} \ell^{(i)} = J_{\mathcal{T}_\phi}(\mathbf{p}^{(i)})^\top \nabla_{w_g^{(i)}} \ell^{(i)}, \quad (4)$$

where $J_{\mathcal{T}_\phi}(\mathbf{p}^{(i)})$ is the Jacobian of \mathcal{T}_ϕ at $\mathbf{p}^{(i)}$.

E.3.2 Bounding the Gradient Difference in $\mathbf{p}^{(i)}$ -Space

Applying Eq. (4) to clients i and j , the difference in their prompt-embedding gradients is

$$\begin{aligned} \left\| \nabla_{\mathbf{p}^{(i)}} \ell^{(i)} - \nabla_{\mathbf{p}^{(j)}} \ell^{(j)} \right\| &= \left\| J_{\mathcal{T}_\phi}(\mathbf{p}^{(i)})^\top \nabla_{w_g^{(i)}} \ell^{(i)} - J_{\mathcal{T}_\phi}(\mathbf{p}^{(j)})^\top \nabla_{w_g^{(j)}} \ell^{(j)} \right\| \\ &\leq \left\| J_{\mathcal{T}_\phi}(\mathbf{p}^{(i)})^\top (\nabla_{w_g^{(i)}} \ell^{(i)} - \nabla_{w_g^{(j)}} \ell^{(j)}) \right\| \\ &\quad + \left\| (J_{\mathcal{T}_\phi}(\mathbf{p}^{(i)})^\top - J_{\mathcal{T}_\phi}(\mathbf{p}^{(j)})^\top) \nabla_{w_g^{(j)}} \ell^{(j)} \right\|. \end{aligned} \quad (5)$$

The first term involves $\nabla_{w_g^{(i)}} \ell^{(i)} - \nabla_{w_g^{(j)}} \ell^{(j)}$, which from Eq. (3) is bounded by

$$\left\| \nabla_{w_g^{(i)}} \ell^{(i)} - \nabla_{w_g^{(j)}} \ell^{(j)} \right\| \leq 2\tau [\kappa(w_1^{(i)}) + \kappa(w_1^{(j)})].$$

The second term depends on how different $J_{\mathcal{T}_\phi}(\mathbf{p}^{(i)})$ is from $J_{\mathcal{T}_\phi}(\mathbf{p}^{(j)})$. Under local Lipschitz assumptions on \mathcal{T}_ϕ , $\|J_{\mathcal{T}_\phi}(\mathbf{p}^{(i)}) - J_{\mathcal{T}_\phi}(\mathbf{p}^{(j)})\|$ can be bounded by some $L' \|\mathbf{p}^{(i)} - \mathbf{p}^{(j)}\|$, and $\|\nabla_{w_g^{(j)}} \ell^{(j)}\| \leq 2\tau \kappa(w_1^{(j)})$.

Hence, a final inequality takes the schematic form:

$$\begin{aligned} \left\| \nabla_{\mathbf{p}^{(i)}} \ell^{(i)} - \nabla_{\mathbf{p}^{(j)}} \ell^{(j)} \right\| &\leq 2\tau [\kappa(w_1^{(i)}) + \kappa(w_1^{(j)})] \|J_{\mathcal{T}_\phi}(\mathbf{p}^{(i)})\| \\ &\quad + 2\tau \kappa(w_1^{(j)}) \|J_{\mathcal{T}_\phi}(\mathbf{p}^{(i)}) - J_{\mathcal{T}_\phi}(\mathbf{p}^{(j)})\|. \end{aligned}$$

Thus, both the condition numbers $\kappa(w_1^{(i)})$ and the local Lipschitz property of \mathcal{T}_ϕ govern gradient differences in prompt-based setups. In particular, if all $w_1^{(i)}$ have $\kappa(w_1^{(i)}) \approx 1$, then these differences remain more tightly controlled, mitigating gradient conflicts during aggregation and often leading to better overall generalization in collaborative training.

E.4 Degree of Freedom in Orthogonal and Block-Orthogonal Transformations

E.4.1 DOF in a General Orthogonal Transformation

An orthogonal matrix $\mathbf{Q} \in \mathbb{R}^{d \times d}$ satisfies the condition:

$$\mathbf{Q}^T \mathbf{Q} = \mathbf{I}_d. \quad (6)$$

This condition imposes $d(d+1)/2$ constraints because the matrix product results in a symmetric identity matrix with d diagonal elements fixed at 1 and $d(d-1)/2$ off-diagonal elements constrained to be zero.

Since an arbitrary $d \times d$ matrix has d^2 independent elements, enforcing orthogonality removes $d(d+1)/2$ degrees of freedom. Thus, the number of free parameters in an orthogonal matrix is:

$$\text{DOF}_{\text{Orthogonal}} = d^2 - \frac{d(d+1)}{2} = \frac{d(d-1)}{2}. \quad (7)$$

E.4.2 DOF in a Block-Orthogonal Transformation

In a block-orthogonal transformation, we divide the matrix $\mathbf{Q} \in \mathbb{R}^{d \times d}$ into r independent orthogonal blocks of size $d/r \times d/r$. Each block \mathbf{Q}_i satisfies the local orthogonality condition:

$$\mathbf{Q}_i^T \mathbf{Q}_i = \mathbf{I}_{d/r}, \quad \forall i \in \{1, \dots, r\}. \quad (8)$$

Since each block acts as an independent $(d/r) \times (d/r)$ orthogonal matrix, the degrees of freedom for each block are:

$$\frac{(d/r)((d/r) - 1)}{2}. \quad (9)$$

With r such blocks, the total degrees of freedom in a block-orthogonal transformation is given by:

$$\text{DOF}_{\text{block-orthogonal}} = r \times \frac{(d/r)((d/r) - 1)}{2} = \frac{d(d/r - 1)}{2}. \quad (10)$$

E.4.3 Condition Number of a Orthogonal Transformation

An orthogonal transformation is represented by a square matrix Q satisfying $Q^T Q = I$. Suppose $Qv = \lambda v$ for some eigenvector v . Taking the inner product, we obtain:

$$\langle Qv, v \rangle = \langle Q^T Qv, Q^T v \rangle = \langle v, Q^T v \rangle.$$

Since $Q^T v = \lambda^{-1}v$, it follows that:

$$\langle Qv, v \rangle = \lambda \langle v, v \rangle, \quad \langle v, Q^T v \rangle = \lambda^{-1} \langle v, v \rangle.$$

Equating both sides yields $\lambda = \pm 1$, confirming that an orthogonal matrix has eigenvalues restricted to $\{\pm 1\}$. As a result, the condition number of Q is fixed at $\kappa(Q) = 1$.

F Experiments

F.1 Setup

F.1.1 Datasets & Baselines

We validate the robustness of our proposed method to domain shift by using five datasets, where each subset has unique domain characteristics. FEMNIST [8] is an extension of the EMNIST [20] dataset. In our study, digit samples (0–9) from four specific users (0, 25, 26, 33) are selected to ensure sufficient data. PACS [42] comprises four distinct domains-Photo, Art painting, Cartoon, and Sketch—each containing seven common classes. VLCS [23] consists of four sub-datasets —VOC2007 [22], LabelMe [67], Caltech101 [25], and SUN09 [18]— each functioning as distinct domains with five categories. Office-Home [74] classifies various commonplace items into 65 categories across four distinct domains: Art, Clipart, Product, and Real-world. TerraIncognita [4] includes wildlife photographs captured by cameras in various locations and four specific locations (L38, L43, L46, L100) are chosen as domains, each encompassing 10 common classes. We divide all subdatasets into three parts according to the following settings: 60% for training, 20% for validation (used for model selection), and 20% for testing.

For baselines, we compare against: FedGH [79], which employs a global header to handle model heterogeneity across diverse clients; FedAKT [45], an adapter-based knowledge-transfer method addressing both statistical and model heterogeneity; and a standard fine-tuning approach, serving as a baseline by allowing full adaptation on client data. These diverse strategies offer a comprehensive evaluation framework, enabling us to assess performance under non-IID, domain-shifted FL conditions.

We also consider three CoCoOp configurations that differ in the architecture and update mechanism of global and local parameters. In CoCoOp (Server CoOp), the global parameters (i.e., textual prompts) and the local parameters (i.e., Meta-Net) are both deployed on the client side, while the server retains only the global prompts. In CoCoOp (Meta-Net Random Init), the server has the same model architecture as the clients, but its Meta-Net remains randomly initialized and is not updated during training in that Meta-Net functions as local parameters. In CoCoOp (All Global), both the textual prompts and Meta-Net are treated as global parameters, and the Meta-Net is also updated along with the prompts through communication between the server and clients.

F.1.2 Implementation Details

For a rigorous method comparison with previous studies [51, 48], we use the CLIP pre-trained model with ViT-B/32 [65]. Since there are performance differences in zero-shot inference based on the initial prompt for each dataset [65], we use "a picture of the number: {class name}" for FEMNIST, and "a picture of a {class name}" for others. We set the local update epoch of the FL process at $E = 1$, and set the number of communication rounds, referred to as T , to be different for each dataset. For PACS, FEMNIST, and VLCS, $T = 200$; and for Office-Home and TerraIncognita, $T = 50$. In the model training process, we utilize cross-entropy loss and the SGD optimizer, with respective hyperparameters for optimizer weight decay and momentum set to $5e - 4$. The learning rates are set to 1×10^{-3} for FEMNIST and 5×10^{-5} for the other datasets. For experiments involving a randomly initialized classifier on Office-Home and TerraIncognita, the learning rates are set to 1×10^{-3} and 1×10^{-4} , respectively.

For CoOp, we set the learnable prompt length M to 4 and 16, and use them as global parameters, while CoCoOp employs the learnable prompt with the length M of 4. We also investigate localized VPT with a global text classifier, varying the visual prompt length p and depth d of the visual prompts to $p = 2, 10$ and $d = 2, 9$ respectively. To determine the optimal block size for FedOT(+b), we conducted experiments with multiple block sizes and recorded the results using the best-performing block size. Given the large number of possible block size options and the time constraints, it was infeasible to evaluate all block sizes across all datasets. Therefore, we employed a random search strategy to identify the best block size for each dataset, except for FEMNIST and Office-Home, where we evaluated multiple block sizes explicitly. The optimal block sizes selected for each dataset are as follows: 256 for FEMNIST, 1 for PACS, 1 for Office-Home, 4 for VLCS, and 16 for TerraIncognita. These values were determined based on experimental results and performance evaluations, ensuring that the selected block sizes maximize the effectiveness of FedOT(+b) for each dataset. We add the softmax activation to the logits to ensure that the output probabilities are scaled between 0 and 1, aiding in the classification task.

Regarding computational resources, we run FedGH, FedAKT, and CoCoOp on OfficeHome using a single NVIDIA A6000 GPU (48GB), and all other experiments on an NVIDIA RTX 3090 GPU (24GB). The total training time varies by dataset and method, ranging from 1.5 to 8 hours for FEMNIST, 6 to 12 hours for PACS, 6.5 to 9.5 hours for OfficeHome, 24 to 30 hours for VLCS, and 10 to 15 hours for Terra. Black-box models such as FedOT and FedCLIP generally require relatively shorter training time compared to other baselines. Meanwhile, FedOT(+B) incurs approximately 2 to 4 times longer training time due to the additional optimization overhead. We use PyTorch 2.1.0 [61] for all experiments.

F.2 Results

F.2.1 Generalization

Dataset	FEMNIST					PACS				
Method	33	0	25	26	AVG	A	C	P	S	AVG
Zero Shot	52.65	50.00	43.75	50.48	49.22	94.38	96.37	99.70	85.86	94.08
CoOp ($M = 4$)	95.10	96.15	97.60	98.08	96.73	94.62	97.44	100.00	86.37	94.61
CoOp ($M = 16$)	95.92	97.12	97.12	97.60	96.94	92.91	96.58	99.10	86.11	93.68
CoCoOp (All Global)	98.37	97.60	96.15	96.15	97.07	93.89	96.58	99.10	86.11	93.92
CoCoOp (Meta-Net Random Init)	34.69	34.13	36.06	38.94	35.96	62.59	79.06	68.56	78.47	72.17
CoCoOp (Server CoOp)	13.88	14.42	9.13	12.50	12.48	86.31	94.02	88.32	87.52	89.04
VPT-SHALLOW ($p = 2$)	70.61	66.83	58.17	76.92	68.13	95.11	97.44	100.00	86.37	94.73
VPT-SHALLOW ($p = 10$)	54.29	54.81	59.13	68.27	59.13	93.64	97.22	100.00	87.39	94.56
VPT-DEEP ($p = 2, d = 2$)	56.73	53.85	41.83	47.12	49.88	93.89	96.79	99.70	84.46	93.71
VPT-DEEP ($p = 10, d = 9$)	48.57	33.65	34.62	31.73	37.14	94.87	97.86	99.70	83.57	94.00
FedAKT (CLIP)	20.50	14.60	4.80	1.90	10.45	8.30	21.40	13.30	18.60	15.40
FedGH (CLIP)	32.00	38.80	40.40	40.40	37.90	44.60	55.60	69.30	49.70	54.80
FedCLIP	77.96	77.40	85.58	79.33	80.07	95.11	96.73	99.70	87.90	94.61
FedAVG	96.73	90.87	90.87	92.31	92.70	95.11	97.01	99.70	86.11	94.48
FedOT	95.92	96.15	92.31	95.19	94.89	95.35	97.44	99.70	86.24	94.68
FedOT+random init	94.29	96.15	96.15	95.19	95.45	86.80	94.44	99.70	83.44	91.10
FedOT+blockwise	97.14	97.60	97.60	99.04	97.85	93.89	97.65	100.00	85.48	94.26

Table 5: The generalization accuracy of FEMNIST and PACS.

Dataset	Office-Home					VLCS					TerraIncognita				
Method	A	C	P	R	AVG	C	L	S	V	AVG	L38	L43	L46	L100	AVG
Zero Shot	78.56	65.86	85.12	87.14	79.17	100.00	63.65	75.15	85.48	81.07	13.16	27.77	20.69	13.54	18.79
CoOp ($M = 4$)	79.59	68.96	87.37	89.21	81.28	98.94	61.21	80.18	86.22	81.64	39.58	35.24	38.02	46.05	39.72
CoOp ($M = 16$)	80.21	69.64	87.94	89.90	81.92	99.29	59.32	79.12	85.78	80.88	37.89	38.36	39.08	37.95	38.32
CoCoOp (All Global)	79.79	67.47	87.49	88.98	80.93	99.65	58.00	76.83	87.11	80.40	38.30	30.26	38.51	36.41	35.87
CoCoOp (Meta-Net Random Init)	62.68	51.89	70.91	70.26	63.94	58.66	44.44	48.48	48.44	50.01	43.06	31.13	29.84	20.31	31.09
CoCoOp (Server CoOp)	75.67	57.62	75.87	87.26	74.11	49.82	46.33	54.42	68.15	54.68	42.40	29.64	30.66	23.59	31.57
VPT-SHALLOW ($p = 2$)	80.82	67.93	86.70	88.98	81.11	99.65	60.83	77.59	86.96	81.26	46.34	41.72	25.18	26.97	35.05
VPT-SHALLOW ($p = 10$)	79.18	67.35	85.57	88.40	80.13	99.65	64.03	76.22	86.07	81.49	43.98	27.27	31.89	15.49	29.66
VPT-DEEP ($p = 2, d = 2$)	79.59	68.61	84.78	87.60	80.15	99.65	58.19	79.12	86.67	80.91	39.73	31.88	39.08	29.85	35.14
VPT-DEEP ($p = 10, d = 9$)	78.35	66.32	83.20	88.75	79.16	99.29	61.02	78.51	86.52	81.34	18.89	33.25	27.23	2.15	20.38
FedAKT (CLIP)	0.83	1.15	2.26	1.38	1.41	65.25	13.96	0.61	29.97	27.45	8.90	1.50	6.20	6.60	5.80
FedGH (CLIP)	0.41	1.61	3.16	1.38	1.64	31.21	44.53	43.29	48.66	41.92	20.90	13.50	0.80	3.70	9.73
FedCLIP	77.94	67.58	87.26	87.83	80.15	100.00	63.09	75.00	87.56	81.41	37.33	32.50	29.03	38.46	34.33
FedAVG	81.65	69.42	86.81	89.32	81.80	99.65	59.13	80.49	89.63	82.23	39.43	33.75	31.56	24.10	32.21
FedOT	80.21	68.73	86.92	89.32	81.30	99.65	59.32	78.96	86.52	81.11	44.34	29.89	42.19	22.77	34.80
FedOT+random init	82.06	71.36	87.49	89.78	82.67	93.64	58.95	79.88	72.00	76.12	34.46	26.40	28.95	18.97	27.20
FedOT+blockwise	82.06	70.90	87.49	89.67	82.53	99.65	61.02	82.93	86.07	82.42	48.85	29.02	27.64	22.15	31.92

Table 6: The generalization accuracy of Office-Home, VLCS, and TerraIncognita.

F.2.2 Personalization

Dataset		FEMNIST				PACS				
Method	Target	0	25	26	AVG	Target	C	P	S	AVG
Zero Shot		50.00	43.75	50.48	48.08		96.37	99.70	85.86	93.98
CoOp ($M = 4$)		97.60	97.60	97.60	97.60		98.72	100.00	93.76	97.49
CoOp ($M = 16$)		98.08	97.60	99.52	98.40		97.86	99.70	92.48	96.68
CoCoOp (All Global)		96.15	97.12	98.08	97.12		98.29	99.40	92.99	96.89
CoCoOp (Meta-Net Random Init)		94.23	97.12	95.67	95.67		98.08	99.40	93.63	97.04
CoCoOp (Server CoOp)		92.31	94.71	94.71	93.91		97.86	100.00	91.34	96.40
VPT-SHALLOW ($p = 2$)		88.94	92.31	91.35	90.87		98.72	100.00	92.23	96.98
VPT-SHALLOW ($p = 10$)		89.90	92.31	91.35	91.19		98.50	100.00	91.85	96.78
VPT-DEEP ($p = 2, d = 2$)		96.63	98.08	98.08	97.60		98.29	100.00	92.61	96.97
VPT-DEEP ($p = 10, d = 9$)	33	88.46	90.87	92.31	90.55	A	98.08	99.70	92.23	96.67
FedAKT (CLIP)		69.90	66.30	57.70	64.63		81.60	81.90	81.60	81.70
FedGH (CLIP)		35.00	38.50	36.50	36.67		76.10	68.70	69.40	71.40
FedCLIP		79.33	85.10	78.37	80.93		98.50	100.00	91.08	96.53
FedAVG		98.56	97.60	97.60	97.92		98.50	100.00	92.36	96.95
FedOT		96.63	96.63	98.56	97.27		98.72	100.00	92.87	97.20
FedOT+random init		96.63	97.12	99.52	97.76		99.36	100.00	92.99	97.45
FedOT+blockwise		98.08	98.56	98.08	98.24		99.36	100.00	93.63	97.66
		33	25	26	AVG		A	P	S	AVG
Zero Shot		52.65	43.75	50.48	48.96		94.38	99.70	85.86	93.31
CoOp ($M = 4$)		96.73	96.15	96.15	96.34		96.58	100.00	93.38	96.65
CoOp ($M = 16$)		96.73	97.60	97.60	97.31		96.33	99.40	92.74	96.16
CoCoOp (All Global)		97.55	98.08	95.67	97.10		95.60	99.40	93.12	96.04
CoCoOp (Meta-Net Random Init)		98.37	97.12	95.67	97.05		95.60	99.40	93.76	96.25
CoCoOp (Server CoOp)		97.14	96.63	95.67	96.48		95.11	100.00	91.21	95.44
VPT-SHALLOW ($p = 2$)		86.94	91.35	91.83	90.04		95.60	100.00	92.74	96.11
VPT-SHALLOW ($p = 10$)		86.12	92.31	91.83	90.09		95.11	100.00	91.72	95.61
VPT-DEEP ($p = 2, d = 2$)		97.14	97.60	98.56	97.77		95.35	99.70	92.23	95.76
VPT-DEEP ($p = 10, d = 9$)	0	86.94	91.35	92.31	90.20	C	95.35	99.70	92.48	95.84
FedAKT (CLIP)		64.80	62.50	56.70	61.33		62.30	81.90	87.50	77.23
FedGH (CLIP)		40.20	39.40	40.40	40.00		46.60	72.90	50.30	56.60
FedCLIP		79.18	85.58	79.81	81.52		94.87	100.00	90.45	95.11
FedAVG		87.76	92.79	92.31	90.95		96.33	99.70	92.74	96.26
FedOT		97.96	96.63	98.56	97.72		95.84	99.70	92.87	96.14
FedOT+random init		97.96	97.60	99.04	98.20		96.33	100.00	93.12	96.48
FedOT+blockwise		97.55	97.12	99.52	98.06		95.35	100.00	93.63	96.33
		33	0	26	AVG		A	P	S	AVG
Zero Shot		52.65	50.00	50.48	48.96		94.38	96.37	85.86	92.20
CoOp ($M = 4$)		95.51	96.63	98.08	96.74		96.09	97.86	93.25	95.73
CoOp ($M = 16$)		97.55	97.12	97.60	97.42		95.60	97.86	92.61	95.36
CoCoOp (All Global)		97.96	97.12	97.12	97.40		95.84	98.29	92.99	95.71
CoCoOp (Meta-Net Random Init)		98.37	93.27	97.12	96.25		95.84	98.50	93.38	95.91
CoCoOp (Server CoOp)		97.55	93.75	93.75	95.02		94.87	97.86	91.21	94.65
VPT-SHALLOW ($p = 2$)		86.53	89.90	91.35	89.26		94.87	98.72	91.97	95.19
VPT-SHALLOW ($p = 10$)		86.94	90.38	91.35	89.56		94.87	98.29	91.85	95.00
VPT-DEEP ($p = 2, d = 2$)		86.94	89.42	92.31	89.56		95.84	98.29	92.36	95.50
VPT-DEEP ($p = 10, d = 9$)	25	86.12	89.42	92.79	89.44	P	94.62	98.08	92.36	95.02
FedAKT (CLIP)		61.50	61.20	65.40	62.70		58.80	85.00	81.60	75.13
FedGH (CLIP)		54.90	43.70	38.50	45.70		53.40	69.20	69.30	60.33
FedCLIP		77.14	81.73	81.73	80.20		95.11	98.72	91.97	95.27
FedAVG		87.35	89.90	91.83	89.69		95.84	98.50	92.61	95.65
FedOT		87.35	89.90	91.83	89.69		95.60	98.72	92.74	95.69
FedOT+random init		98.37	97.60	98.08	98.02		96.33	98.93	94.27	96.00
FedOT+blockwise		97.55	98.56	99.52	98.54		95.60	98.93	92.99	96.27
		33	0	25	AVG		A	C	P	AVG
Zero Shot		52.65	50.00	43.75	48.80		94.38	96.37	99.70	96.82
CoOp ($M = 4$)		95.92	97.12	98.08	97.04		95.11	98.29	100.00	97.80
CoOp ($M = 16$)		96.73	97.60	97.12	97.15		95.84	97.86	100.00	97.90
CoCoOp (All Global)		97.96	95.67	96.15	96.59		95.60	98.50	100.00	98.03
CoCoOp (Meta-Net Random Init)		94.69	94.71	96.63	95.34		95.60	98.29	99.40	97.76
CoCoOp (Server CoOp)		97.14	93.75	96.63	95.84		95.35	98.50	100.00	97.95
VPT-SHALLOW ($p = 2$)		97.55	97.12	97.12	97.26		95.11	98.93	99.70	97.91
VPT-SHALLOW ($p = 10$)		86.53	89.90	91.83	89.42		94.62	98.29	99.70	97.54
VPT-DEEP ($p = 2, d = 2$)		97.55	97.60	97.12	97.42		94.87	98.29	99.70	97.62
VPT-DEEP ($p = 10, d = 9$)	26	86.53	87.98	91.35	88.62	S	94.87	97.86	99.70	97.48
FedAKT (CLIP)		73.80	78.60	72.10	74.83		59.30	85.00	80.10	74.80
FedGH (CLIP)		46.70	34.00	40.40	40.37		56.40	71.40	66.90	64.90
FedCLIP		79.59	79.81	86.06	81.82		95.35	97.65	100.00	97.67
FedAVG		87.35	89.90	91.83	89.69		95.60	98.72	99.70	98.01
FedOT		97.55	97.12	96.63	97.10		95.35	98.72	99.70	97.92
FedOT+random init		98.78	97.12	97.12	97.67		95.84	98.72	100.00	98.19
FedOT+blockwise		97.96	98.08	97.12	97.72		96.58	98.72	99.70	98.33

Table 7: The personalization accuracy of FEMNIST and PACS.

Dataset	Office-Home					VLCS					TerraIncognita				
Method	Target	C	P	R	AVG	Target	L	S	V	AVG	Target	L43	L46	L100	AVG
Zero Shot	A	65.86	85.12	87.14	79.37	C	63.65	75.15	85.48	74.76	L38	27.77	20.69	13.54	20.67
CoOp ($M = 4$)		77.09	89.97	90.24	85.77		72.13	87.80	90.22	83.38		53.55	57.89	67.38	59.61
CoOp ($M = 16$)		76.29	90.19	89.90	85.46		72.50	84.60	89.04	82.05		53.92	59.12	64.82	59.29
CoCoOp (All Global)		72.85	88.16	88.98	83.33		70.06	84.60	91.56	82.07		46.58	54.37	64.62	55.19
CoCoOp (Meta-Net Random Init)		73.31	88.05	89.09	83.48		80.23	85.82	89.33	85.13		61.64	59.69	79.59	66.97
CoCoOp (Server CoOp)		71.25	88.50	87.72	82.49		78.34	85.82	91.26	85.14		58.53	62.31	72.41	64.42
VPT-SHALLOW ($p = 2$)		71.25	88.61	88.98	82.95		76.84	86.28	90.22	84.45		59.65	58.79	71.90	63.45
VPT-SHALLOW ($p = 10$)		68.50	87.71	88.52	81.58		75.33	85.37	89.63	83.44		55.67	57.89	68.72	60.76
VPT-DEEP ($p = 2, d = 2$)		70.33	88.39	87.83	82.18		78.91	86.13	89.63	84.89		59.78	60.67	73.64	64.70
VPT-DEEP ($p = 10, d = 9$)		66.32	86.81	87.72	80.28		79.85	84.76	90.81	85.14		54.67	58.38	72.82	61.96
FedAKT (CLIP)		22.48	31.38	26.67	26.84		63.02	64.94	62.61	63.52		41.60	41.40	71.90	51.63
FedGH (CLIP)		1.38	3.16	2.30	2.28		45.66	44.82	32.05	40.84		0.00	0.20	3.50	1.23
FedCLIP		68.50	87.49	88.17	81.39		68.55	80.18	88.44	79.06		32.75	41.86	40.41	38.34
FedAVG		75.14	90.42	90.01	85.19		73.82	85.98	89.63	83.14		55.79	61.24	69.13	62.05
FedOT		76.40	90.87	90.24	85.84		75.52	85.82	89.93	83.76		61.39	63.61	76.51	67.17
FedOT+random init		81.10	93.35	91.39	88.61		82.49	86.59	77.19	82.09		58.66	61.41	77.03	65.70
FedOT+blockwise	80.64	93.46	90.93	88.34	81.17	86.89	90.52	86.19	60.90	65.09	77.74	67.91			
Zero Shot	C	A	P	R	AVG	L	C	S	V	AVG	L43	L38	L46	L100	AVG
CoOp ($M = 4$)		78.56	85.12	87.14	83.61		100.00	75.15	85.48	86.88		13.16	20.69	13.54	15.80
CoOp ($M = 16$)		84.12	89.63	90.47	88.07		100.00	88.26	91.11	93.12		66.97	53.80	69.13	63.30
CoOp ($M = 16$)		82.06	89.29	91.04	87.46		99.65	85.67	90.67	92.00		62.42	54.87	71.49	62.93
CoCoOp (All Global)		80.82	87.60	88.63	85.68		100.00	84.30	89.63	91.31		63.70	50.04	62.56	58.77
CoCoOp (Meta-Net Random Init)		80.62	88.05	88.86	85.84		100.00	85.82	89.78	91.87		74.14	59.28	79.18	70.87
CoCoOp (Server CoOp)		80.00	88.39	87.37	85.25		99.65	85.82	91.11	92.19		75.17	60.18	73.74	69.70
VPT-SHALLOW ($p = 2$)		80.82	88.16	89.09	86.02		99.65	86.59	90.07	92.10		63.59	60.51	74.56	66.22
VPT-SHALLOW ($p = 10$)		77.11	87.94	89.32	84.79		98.94	85.53	90.52	91.66		63.03	51.51	73.64	62.73
VPT-DEEP ($p = 2, d = 2$)		80.41	88.39	88.75	85.85		100.00	85.82	89.63	91.82		64.46	54.87	75.49	64.94
VPT-DEEP ($p = 10, d = 9$)		77.53	86.36	87.94	83.94		100.00	86.59	90.52	92.37		63.49	58.05	73.85	65.13
FedAKT (CLIP)		22.31	41.53	28.97	30.94		82.98	64.94	63.80	70.57		61.40	46.50	66.30	58.07
FedGH (CLIP)		2.48	2.26	2.76	2.50		94.33	44.51	48.37	62.40		4.60	10.30	0.00	4.97
FedCLIP		77.97	86.81	87.72	84.17		100.00	79.12	88.30	89.14		44.50	35.57	38.97	39.68
FedAVG		84.12	89.52	89.78	87.81		99.65	86.43	90.67	92.25		69.12	50.53	68.92	62.86
FedOT		82.89	90.53	90.47	87.96		99.65	86.74	90.81	92.40		76.96	54.78	80.92	70.89
FedOT+random init	85.36	92.67	91.16	89.73	96.47	86.89	76.89	86.75	74.65	58.14	77.74	70.18			
FedOT+blockwise	84.33	92.67	91.04	89.35	100.00	87.20	90.37	92.52	75.68	58.63	79.90	71.40			
Zero Shot	P	A	C	R	AVG	S	C	L	V	AVG	L46	L38	L43	L100	AVG
CoOp ($M = 4$)		78.56	65.86	87.14	77.19		100.00	63.65	85.48	83.04		13.16	27.77	13.54	18.16
CoOp ($M = 4$)		84.33	74.23	89.90	82.82		100.00	75.89	90.07	88.65		62.83	46.45	72.62	60.63
CoOp ($M = 16$)		85.36	75.83	90.59	83.93		99.65	77.97	88.00	88.54		63.75	50.81	67.90	60.82
CoCoOp (All Global)		79.59	72.16	89.09	80.28		100.00	76.65	89.93	88.86		65.39	43.84	65.23	58.15
CoCoOp (Meta-Net Random Init)		79.79	73.08	89.21	80.69		100.00	79.47	89.48	89.65		74.04	60.77	78.77	71.19
CoCoOp (Server CoOp)		80.00	71.25	87.14	79.46		99.65	79.85	90.96	90.15		73.99	57.66	73.64	68.43
VPT-SHALLOW ($p = 2$)		79.59	70.56	89.32	79.82		100.00	80.98	89.93	90.30		69.43	52.55	77.44	66.47
VPT-SHALLOW ($p = 10$)		76.91	66.55	88.40	77.29		100.00	80.23	88.30	89.51		63.03	54.92	75.08	64.34
VPT-DEEP ($p = 2, d = 2$)		79.59	68.73	88.17	78.83		100.00	80.79	89.33	90.04		64.41	58.16	77.23	66.60
VPT-DEEP ($p = 10, d = 9$)		77.11	64.15	86.68	75.98		99.65	79.47	89.48	89.53		63.85	53.05	65.23	60.71
FedAKT (CLIP)		22.73	20.41	24.60	22.58		91.49	58.87	56.68	69.01		66.40	36.40	43.90	48.90
FedGH (CLIP)		0.83	0.92	2.53	1.43		90.78	44.91	49.26	61.65		3.90	5.20	7.80	5.63
FedCLIP		77.73	68.16	87.83	77.91		100.00	72.88	87.41	86.76		45.67	30.39	45.74	40.60
FedAVG		82.89	74.80	90.01	82.57		100.00	77.21	89.93	89.05		70.40	53.67	74.05	66.04
FedOT		82.89	76.63	90.01	83.18		100.00	81.73	89.93	90.55		75.93	61.02	78.67	71.87
FedOT+random init	85.15	81.44	90.82	85.80	100.00	82.11	89.63	90.58	74.65	58.90	75.38	69.64			
FedOT+blockwise	84.95	80.64	91.04	85.54	100.00	82.11	90.81	90.97	75.68	59.03	80.62	71.78			
Zero Shot	R	A	C	P	AVG	V	C	L	S	AVG	L100	L38	L43	L46	AVG
CoOp ($M = 4$)		78.56	65.86	85.12	76.51		100.00	63.65	75.15	79.60		13.16	27.77	20.69	20.54
CoOp ($M = 4$)		84.95	76.40	89.29	83.55		99.65	74.20	86.28	86.71		64.00	50.93	57.65	57.53
CoOp ($M = 16$)		83.09	75.83	89.29	82.74		99.29	74.95	83.23	85.82		61.65	55.67	57.32	58.21
CoCoOp (All Global)		80.41	72.85	88.28	80.51		99.65	75.52	85.06	86.74		63.49	48.19	52.74	54.81
CoCoOp (Meta-Net Random Init)		80.62	73.42	88.05	80.70		100.00	79.66	86.89	88.85		74.30	62.76	58.54	65.20
CoCoOp (Server CoOp)		79.79	71.82	88.39	80.00		99.65	79.47	86.13	88.42		73.84	57.04	61.57	64.15
VPT-SHALLOW ($p = 2$)		79.18	71.82	88.50	79.83		99.65	79.66	86.43	88.58		62.26	55.29	62.71	60.09
VPT-SHALLOW ($p = 10$)		76.08	67.24	87.82	77.05		99.65	79.85	86.59	88.70		62.31	52.68	55.19	56.73
VPT-DEEP ($p = 2, d = 2$)		80.62	69.42	88.28	79.44		99.65	81.36	85.67	88.89		62.83	58.03	63.21	61.36
VPT-DEEP ($p = 10, d = 9$)		77.53	65.52	86.13	76.39		99.65	79.66	84.60	87.97		53.15	47.07	54.13	51.45
FedAKT (CLIP)		21.90	26.83	37.02	28.58		89.36	63.40	69.21	62.99		59.50	32.20	44.20	45.30
FedGH (CLIP)		1.24	1.15	2.93	1.68		90.78	46.42	44.51	57.59		16.30	8.50	9.50	9.50
FedCLIP		77.73	68.04	87.26	77.68		100.00	69.68	78.35	82.68		48.49	36.24	41.14	41.96
FedAVG		83.92	75.03	89.85	82.93		99.65	73.82	85.98	86.48		69.84	52.80	57.73	60.12
FedOT		82.68	77.32	90.64	83.55		99.65	77.78	85.98	87.80		75.27	57.53	64.51	65.77
FedOT+random init	84.95	81.21	93.35	86.50	96.11	81.54	87.04	88.23	62.42	52.93	57.97	57.77			
FedOT+blockwise	84.12	81.44	94.02	87.31	99.65	81.73	87.20	89.53	72.50	57.29	64.27	64.69			

Table 8: The personalization accuracy of Office-Home, VLCS, and TerraIncognita.

F.2.3 Comprehensive

Dataset	FEMNIST					PACS				
Method	33	0	25	26	AVG	A	C	P	S	AVG
Zero Shot	52.65	50.00	43.75	50.48	49.22	94.38	96.37	99.70	85.86	94.08
CoOp ($M = 4$)	96.98	96.30	96.96	97.30	96.88	96.78	96.85	96.80	94.94	96.34
CoOp ($M = 16$)	97.78	97.26	97.35	97.26	97.41	95.74	96.26	96.29	94.95	95.81
CoCoOp (All Global)	97.43	97.23	97.09	96.48	97.06	96.14	96.18	96.56	95.05	95.98
CoCoOp (Meta-Net Random Init)	80.43	81.32	81.21	81.24	81.05	88.43	91.96	89.07	92.94	90.60
CoCoOp (Server CoOp)	73.90	75.97	73.55	75.01	74.60	93.88	95.09	93.07	95.34	94.34
VPT-SHALLOW ($p = 2$)	85.80	84.24	81.49	92.18	85.93	96.52	96.45	96.39	95.03	96.09
VPT-SHALLOW ($p = 10$)	81.96	81.27	81.95	84.13	82.33	96.00	96.01	96.25	95.00	95.82
VPT-DEEP ($p = 2, d = 2$)	87.38	86.79	77.63	84.85	84.16	96.20	96.02	96.55	94.33	95.77
VPT-DEEP ($p = 10, d = 9$)	80.05	76.06	75.74	74.40	76.56	96.22	96.35	96.19	94.00	95.69
FedAKT (CLIP)	53.60	49.65	48.23	56.60	52.02	63.35	63.28	59.68	60.75	61.76
FedGH (CLIP)	35.50	39.70	44.38	40.38	39.99	71.40	56.60	60.33	64.90	61.18
FedCLIP	80.19	80.49	81.55	81.20	80.86	96.17	95.26	96.38	95.23	95.76
FedAVG	97.62	90.93	89.99	90.35	92.22	96.49	96.45	96.66	95.03	96.16
FedOT	96.94	97.33	90.35	96.62	95.31	96.74	96.46	96.69	95.00	96.22
FedOT+random init	96.89	97.69	97.55	97.05	97.30	94.79	95.97	96.93	94.50	95.55
FedOT+blockwise	97.97	97.95	98.31	98.05	98.07	96.72	96.66	97.20	95.12	96.42

Table 9: The comprehensive accuracy of FEMNIST and PACS.

Dataset	Office-Home					VLCS					TerraIncognita				
Method	A	C	P	R	AVG	C	L	S	V	AVG	L38	L43	L46	L100	AVG
Zero Shot	78.56	65.86	85.12	87.14	79.17	100.00	63.65	75.15	85.48	81.07	13.16	27.77	20.69	13.54	18.79
CoOp ($M = 4$)	84.22	83.30	83.96	84.96	84.11	87.27	85.15	86.54	86.59	86.39	54.60	56.29	54.98	54.66	55.13
CoOp ($M = 16$)	84.15	83.01	84.93	84.53	84.15	86.36	83.83	86.19	85.81	85.55	53.94	56.79	55.39	53.15	54.81
CoCoOp (All Global)	82.45	81.13	82.08	82.63	82.07	86.47	82.98	85.85	86.84	85.53	50.97	51.64	53.24	50.21	51.51
CoCoOp (Meta-Net Random Init)	78.28	77.36	78.25	78.09	77.99	78.51	80.01	79.36	78.75	79.16	61.00	60.93	60.86	53.98	59.19
CoCoOp (Server CoOp)	80.79	78.35	78.57	81.82	79.88	76.31	80.73	81.22	83.35	80.40	58.91	59.68	58.99	54.01	57.90
VPT-SHALLOW ($p = 2$)	82.42	81.50	81.54	82.12	81.89	88.25	84.29	87.13	88.18	86.96	59.17	60.10	56.15	51.81	56.81
VPT-SHALLOW ($p = 10$)	80.98	80.43	79.36	79.89	80.16	87.50	84.75	86.19	88.04	86.62	56.57	53.86	56.23	46.42	53.27
VPT-DEEP ($p = 2, d = 2$)	81.54	81.54	80.32	81.48	81.22	88.58	83.41	87.31	88.34	86.91	58.46	56.68	59.72	53.48	57.08
VPT-DEEP ($p = 10, d = 9$)	79.80	79.54	77.79	79.48	79.15	88.68	84.53	86.78	87.61	86.90	51.19	57.16	52.34	39.13	49.95
FedAKT (CLIP)	20.34	23.49	17.50	21.78	20.78	63.96	56.42	51.91	62.99	58.82	40.95	43.93	38.23	35.63	39.68
FedGH (CLIP)	1.81	2.28	1.86	1.68	1.91	38.44	57.94	57.06	57.59	52.76	6.15	7.10	4.43	9.50	6.79
FedCLIP	80.53	80.02	80.25	80.22	80.25	84.29	82.63	83.82	83.90	83.66	38.09	37.89	37.71	40.07	38.44
FedAVG	84.31	83.21	83.63	84.53	83.92	87.27	83.97	86.91	87.27	86.35	56.40	55.58	57.42	51.12	55.13
FedOT	84.43	83.16	84.11	84.99	84.17	87.73	84.13	87.66	87.48	86.75	61.46	60.64	64.45	55.02	60.39
FedOT+random init	86.98	85.14	86.23	87.32	86.42	84.98	79.80	87.91	84.17	84.21	57.89	59.23	59.47	48.07	56.17
FedOT+blockwise	86.77	84.74	86.03	87.31	86.21	89.56	84.65	88.96	88.66	87.96	63.15	60.81	60.74	54.05	59.69

Table 10: The comprehensive accuracy of Office-Home, VLCS, and TerraIncognita.

G Ablation

G.1 Robustness to Communication Rounds.

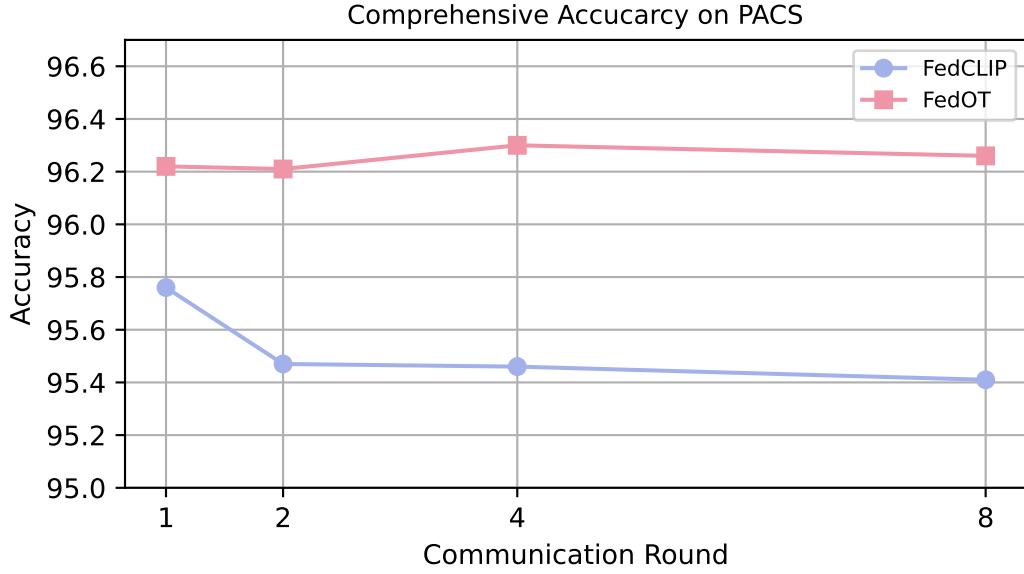


Figure 4: Comparison of comprehensive accuracy on PACS across different communication rounds using FedOT and FedCLIP.

G.2 Multi-Client Scenario

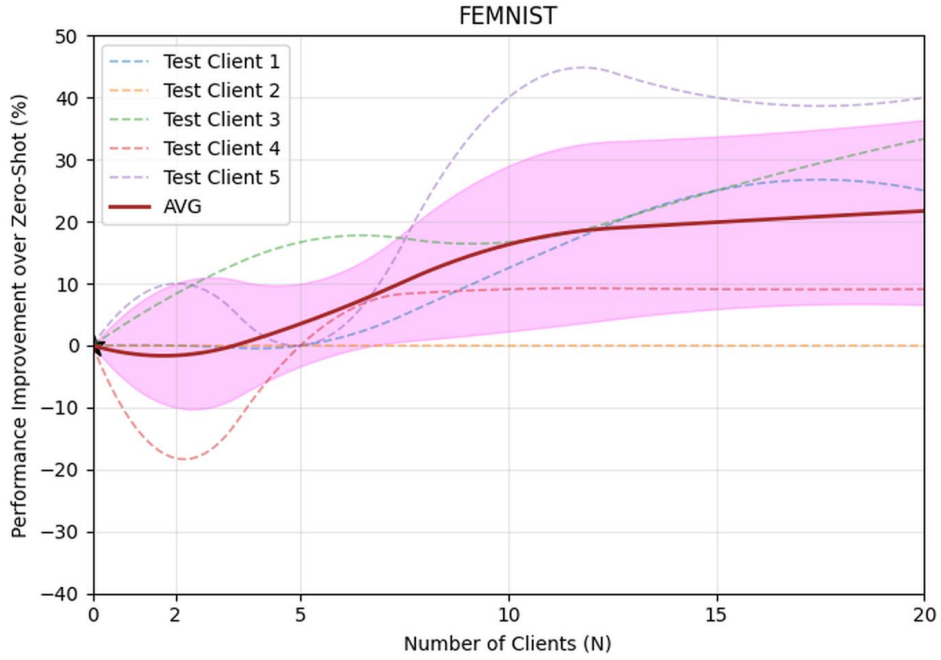


Figure 5: Average performance improvement of test clients in a multi-client scenario. The x-axis shows the number of training clients, while the y-axis indicates the average performance enhancement compared to CLIP’s zero-shot performance.

H Social Impact

Our proposed framework offers significant societal benefits by enhancing both data privacy and model intellectual property in AI systems. For users, it enables personalized AI services without requiring direct data sharing, thereby protecting sensitive information while delivering tailored experiences. For service providers, the framework preserves model privacy by concealing proprietary architectures. It also facilitates learning from user feedback without direct access to user data, effectively simulating data exposure without compromising privacy. By addressing these security concerns, our approach fosters ethical AI development, strengthens trust between users and service providers, and encourages the adoption of data-secure and IP-respecting AI solutions in real-world applications.